

Origin and evolution of lago Yehuín (Tierra del Fuego, Argentina): Results from a geophysical survey

***Jorge G. Lozano¹, Alejandro Tassone¹, Emanuele Lodolo², Marco Menichetti³,
María E. Cerredo¹, Donald M. Bran¹, Federico Esteban¹, Juan P. Ormazabal¹,
Luca Baradello², Juan F. Vilas¹**

¹ CONICET-Instituto de Geociencias Básicas, Aplicadas y Ambientales de Buenos Aires (IGeBA), Departamento de Ciencias Geológicas, Facultad de Ciencias Exactas y Naturales, Universidad de Buenos Aires, Ciudad Universitaria, C1428EHA, Buenos Aires, Argentina. jorgegabriellozano@gmail.com; tassoneale@yahoo.com.ar; marycerredo@gmail.com; donalddmbran@gmail.com; federico.esteban@gmail.com; juanpablo_ormazabal@hotmail.com; vilas@gl.fcen.uba.ar

² Istituto Nazionale di Oceanografia e di Geofisica Sperimentale (OGS), Borgo Grotta Gigante 42/c, 34010 Sgonico, Trieste, Italy. elodolo@inogs.it; lbaradello@inogs.it

³ Dipartimento di Scienze della Terra, Vita e dell'Ambiente dell'Università di Urbino Campus Scientifico E. Mattei, 61020 Urbino (FU), Italy. marco.menichetti@uniurb.it

* Corresponding author: jorgegabriellozano@gmail.com

ABSTRACT. Lago Yehuín, a WNW-ESE elongated basin located in the outer fold-and-thrust belt of the Fuegian Andes, occupies a compartmented structural depression originated along a segment of the left-lateral Lago Deseado fault system. This paper describes the first geophysical survey performed within the lake. New acquired high-resolution single-channel seismic data, integrated with geological information in the surroundings of the Lago Yehuín, allowed to: (i) produce a complete bathymetric map of the lake, (ii) reconstruct the basement surface of the lake, and (iii) analyze the geometry, distribution, and thickness of the sedimentary infill. Two sub-basins were recognized within Lago Yehuín: A western sub-basin, 7.5 km long, with a maximum depth of 118 m; an eastern sub-basin, 7.2 km long with a maximum depth of 80 m. Both sub-basins are limited by a set of normal faults which overprint NE-verging thrusts. Three seismostratigraphic units have been identified in the seismic records: (1) a lower unit with wedged geometry interpreted as a mass flow deposits; (2) a thick (up to 120 m) intermediate unit of glacio-lacustrine nature and irregularly distributed in the Yehuín basin; (3) a thin (generally <10 m) upper lacustrine unit which drapes the entire basin. Lago Yehuín is considered a Neogene basin generated by strike-slip tectonics that was later affected by glacial and glacio-lacustrine deposition. Interpreted submerged ridge moraines within Lago Yehuín are correlated with onland moraine arcs built by the complete recessional paths of Fuego and Ewan ice lobes. A significant structural control is proposed not only for the formation of Lago Yehuín, but also for the general paths of the northern arms of the Fagnano palaeo-glacier.

Keywords: Lago Yehuín, Fuegian Andes, Single-channel seismic profiles, Strike-slip tectonics.

RESUMEN. Origen y evolución del lago Yehuín (isla Grande de Tierra del Fuego, Argentina): resultados de un relevamiento geofísico. El lago Yehuín, una cuenca elongada de rumbo ONO-ESE localizada en la faja plegada y corrida externa de los Andes Fueguinos, ocupa una depresión compartimentada originada a lo largo de un segmento del sistema de fallas sinistralas del lago Deseado. Este trabajo describe un primer relevamiento geofísico llevado a cabo en el lago. Los datos de sísmica monocanal de alta resolución, integrados con información geológica de los alrededores del lago Yehuín, permitieron: (i) producir un mapa de la batimetría completa del lago, (ii) reconstruir la superficie del basamento del lago, y (iii) analizar la geometría, distribución y espesor del relleno sedimentario. Se reconocieron dos subcuencas dentro del lago Yehuín: una subcuenca oeste de 7,5 km de largo, con una profundidad máxima de 118 m; una subcuenca este de 7,2 km de largo y una profundidad máxima de 80 m. Ambas subcuencas están limitadas por

un conjunto de fallas normales que cortan a una serie de corrimientos de vergencia NE. Se identificaron tres unidades sísmo-estratigráficas en el registro sísmico: (1) una unidad inferior con geometría acuñada interpretada como depósitos de remoción en masa; (2) una unidad intermedia gruesa (de hasta 120 m) de origen glaciolacustre e irregularmente distribuida en la cuenca del lago; (3) una unidad superior lacustre delgada (<10 m) que cubre la cuenca entera. El lago Yehuín se considera una cuenca neógena e origen tectónico que fue luego afectada por depositación glaciaria y glaciolacustre. Se han interpretado morenas sumergidas dentro del lago Yehuín que se correlacionan con los arcos morrénicos en tierra y permiten completar el camino recesivo de los lóbulos de hielo Ewan y Fuego. Se propone un fuerte control estructural no solo para la formación del lago Yehuín, sino también para las rutas generales de los brazos norte del Paleoglaciario Fagnano.

Palabras clave: Lago Yehuín, Andes Fueguinos, Perfiles sísmicos monocanal, Tectónica de rumbo.

1. Introduction

Lago Yehuín (LY) is located in the southernmost Andes, in isla Grande de Tierra del Fuego (Fig. 1). The regional geologic history of this area encompasses several tectonic phases which include a Late Jurassic-Early Cretaceous extension, a Late Cretaceous-Palaeogene compression, and strike-slip tectonics during the Neogene (Katz, 1972; Dalziel *et al.*, 1974; Dalziel and Palmer, 1979; Kohn *et al.*, 1995; Klepeis, 1994a, b; Kraemer *et al.*, 1996; Kraemer, 2003; Lodolo *et al.*, 2003).

LY is a lacustrine basin located 10 km north of lago Fagnano, the largest freshwater lake of Tierra del Fuego, which occupies a pull-apart basin developed within the South America-Scotia transform boundary (Fuenzalida, 1972; Dalziel, 1989; Lodolo *et al.*, 2003). LY, which displays a WNW-ESE oriented elongated shape, lays in a low altitude zone (between 900 and 50 m a.s.l.) and is part of a provincial reserve named “Corazón de la Isla”. The lake is the largest freshwater lacustrine body within the reserve, and the largest basin within the Fuegian steppe, with a surface of 43 km². The mean

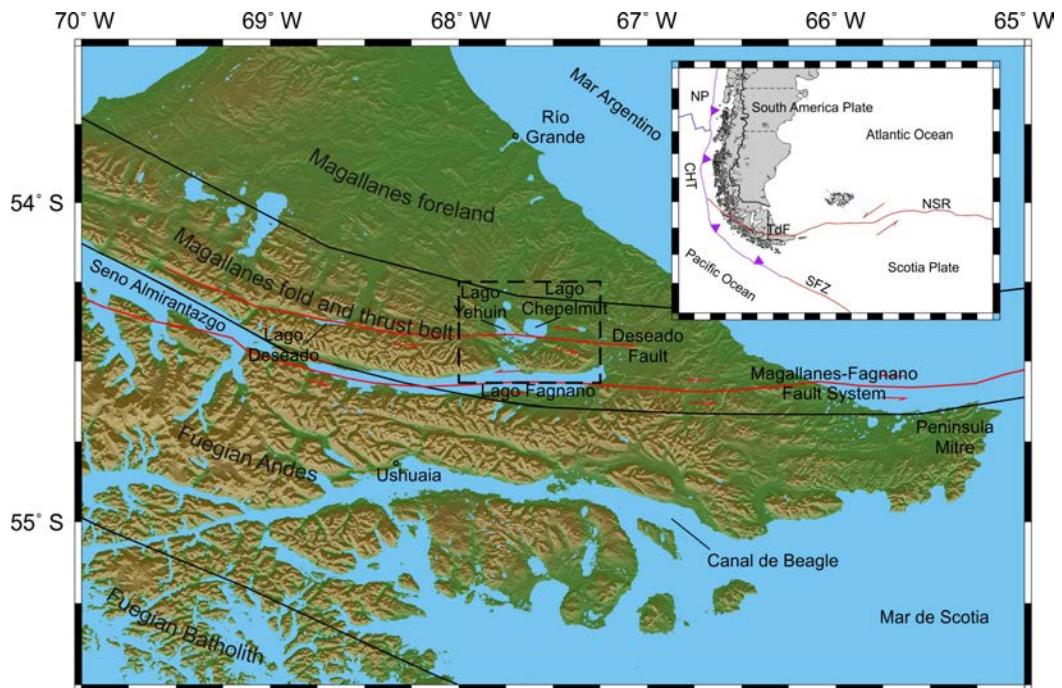


FIG. 1. Physiographic and structural provinces of the Isla Grande de Tierra del Fuego. In the inset box, the current plate tectonic frame of the southern tip of South American, Scotia and Antarctic Plates; **NP**: Nazca Plate; **CHT**: Chile Trench; **TdF**: Tierra del Fuego; **NSR**: North Scotia Ridge; **SFZ**: Shackleton Fracture Zone. The black dashed box limits the studied area SFZ (Fig. 2).

annual precipitation and temperature are 600 mm and 6 °C, respectively. The Río In is the main river which brings water from the neighboring Lago Chepelmut into lago Yehuín. The output waters of LY derive to the lago Yakush, a small lake located a few kilometers to the south (Fig. 2).

In the last ten years, a series of geophysical and geological surveys have been conducted in the Tierra del Fuego region, focusing primarily in the tectonic evolution of the South America-Scotia plate during the Cenozoic, and analyzing the features associated with this continental transform margin (Esteban *et al.*, 2011, 2014; Lippai *et al.*, 2004; Lodolo *et al.*, 2003, 2007; Menichetti *et al.*, 2001, 2007a and b, 2008; Tassone *et al.*, 2005, 2011). Several works, mainly of geophysical nature, have been devoted to other Fuegian lakes, like lago Fagnano (Lippai *et al.*, 2004; Zanolla *et al.*, 2011; Waldmann *et al.*, 2008, 2009,

2010a and b, 2011; Esteban *et al.*, 2014) and lago Roca (Lodolo *et al.*, 2010). Only general references are found about LY, which was considered as the result of glacial activity (Coronato *et al.*, 2008a).

The main objective of this study is to decipher the genesis of the LY basin and reconstruct the geometry of the sedimentary infill by means of the interpretation of the first seismic survey performed within the lake. About 39 km of high-resolution seismic profiles have been acquired with a Boomer sub-bottom profiler; these data have been used to present a bathymetric map of the lake, to identify the bedrock and characterize the sedimentary infill of the basin. The data allowed to derive the depositional architecture and thickness of the deposits within the lake, and analyze the possible relationship between pre-existing structures and the recent sedimentary setting. The results were

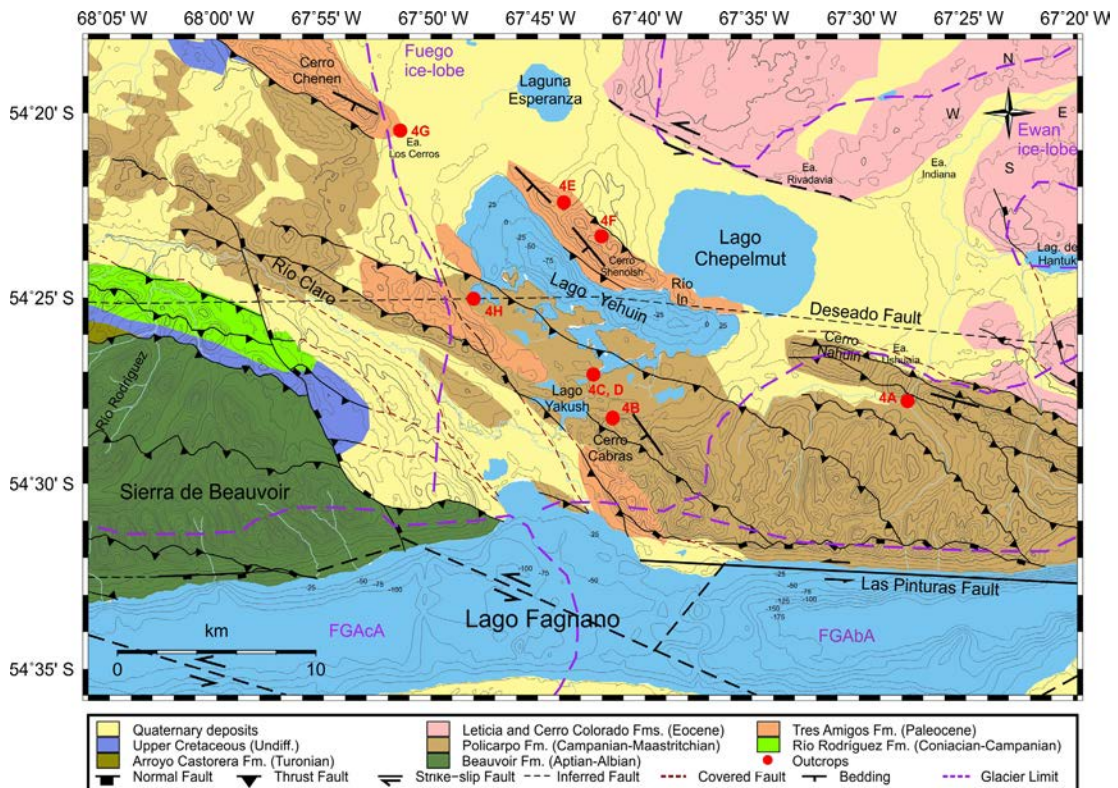


FIG. 2. Geologic map of the lago Yehuín area; location in figure 1. The elevations of the bottom of lago Yehuín (new acquired data) and lago Fagnano are displayed. Las Pinturas fault is part of the Magallanes-Fagnano Fault Zone. Adapted from Menichetti *et al.* (2008); Martinioni *et al.* (2013); Torres-Carbonell *et al.* (2013) and Esteban *et al.* (2014). The red dots show the position of studied outcrops, with the reference to the respective figures. The purple dashed line encloses the area of Fagnano Glacier, Fuego and Ewan glacier lobes after Coronato *et al.* (2009); FG AcA: Fagnano glacier accumulation area; FG AbA: Fagnano glacier ablation area.

integrated with geologic information from the surrounding areas in order to present a model for the LY origin and evolution.

2. Geologic and tectonic framework of the lago Yehuín area

The geologic history of the southernmost Andes is the product of a complex succession of contrasting tectonic regimes. During Early Mesozoic the active margin of Gondwanaland stretched between the adjacent southern South America-Antarctic Peninsula and the Pacific margin (Dalziel and Elliot, 1973; Dalziel, 1982). A major tectonic event was a widespread extensional regime in the Late Jurassic and related silicic volcanic activity that led to the formation of the Rocas Verdes marginal basin along the southern Patagonian and Fuegian continental margin (Dalziel *et al.*, 1974; Suárez and Pettigrew, 1976; Hanson and Wilson, 1991; Calderón *et al.*, 2007). Widespread extensional fault arrays consisting of N- to NW-oriented grabens and half-grabens and E- to NE-oriented transfer faults are associated with this Jurassic stage (Ghiglione *et al.*, 2013).

In the Late Cretaceous, compression along the Pacific margin of the South American plate led to the closure and inversion of the marginal basin and the development of the Andean orogen with its associated fold-and-thrust belt (Dalziel *et al.*, 1974; Wilson, 1991; Bruhn, 1979; Nelson *et al.*, 1980; Diraison *et al.*, 2000; Kraemer, 2003; Menichetti *et al.*, 2008).

Since the Late Oligocene-Early Miocene the tectonics shifted to a strike-slip regime in correspondence to the formation of the Scotia Plate and its boundary with the South America Plate, represented in the southernmost Andes by the Magallanes-Fagnano fault system (MFFS; Klepeis and Austin, 1997; Diraison *et al.*, 2000; Lodolo *et al.*, 2003; Ghiglione and Ramos, 2005). Since then, this transform boundary accommodates the relative movement between the South America and Scotia plates. The associated structures are mainly transtensional with extensional faults and the development of pull-apart basins along the main wrench faults (Lodolo *et al.*, 2003; Menichetti *et al.*, 2008). The Lago Deseado Fault System (LDFS, Fig. 1) is one of the major satellite structures associated with the plate boundary. LDFS is a linear structure about 100 km long with a left-lateral movement and

associated extensional component (Klepeis, 1994b) which runs across the studied area.

From a structural point of view, the southernmost Andes can be divided into several WNW-ESE trending morphostructural provinces (Kranck, 1932; Winslow, 1982; Dalziel and Brown, 1989; Suárez *et al.*, 2000; Olivero and Martinioni, 2001; Klepeis and Austin, 1997; Diraison *et al.*, 2000; Kraemer, 2003; Menichetti *et al.*, 2008, Fig. 1):

- (i) The most internal province, which stretches between the forearc active ocean/continent convergent margin of the Chile Trench and the accretionary wedge in the Pacific Ocean.
- (ii) The Fuegian Batholith, comprising the Late Cretaceous plutons emplaced at mid to upper crustal levels into a low-grade metamorphic complex.
- (iii) The Fuegian Cordillera, composed of Palaeozoic metamorphic rocks-sedimentary and magmatic remnants of the Rocas Verdes basin, characterized by NE verging thrust complexes; it represents the thick skinned, or internal, Fuegian fold-and-thrust-belt (FFTB).
- (iv) The external province, which includes the Magallanes foreland-thrust belt-thin skinned FFTB or external FFTB-which is located north of the seno Almirantazgo and lago Fagnano, across the central-northern part of the Island (Fig. 1). The Magallanes foreland basin is filled with Cenozoic sediments involved in shallow NNE-verging thrust systems. The studied area is set within this morphostructural province.

The main structural features of the LY area are N-NE-verging thrusts, with a morphology characterized by elongated NW-SE valleys. In map view, the shape of the lake basin broadly mimics the trend of local thrusts (Fig. 2). A series of NW-SE normal faults related to the strike-slip tectonics cut across the thrust faults in the western area, near the Río Claro mouth.

The central part of the Tierra del Fuego island, north of Lago Fagnano, includes a succession of Lower Cretaceous to Eocene units exposed along WNW-ESE oriented belts (Fig. 3; Malumián and Olivero, 2006; Olivero and Malumián, 2008; Martinioni *et al.*, 2013). The Lower Cretaceous Beauvoir Formation exposed along the northern margin of Lago Fagnano, part of the back-arc basin-fill of the former Rocas Verdes marginal basin, is composed of slates, mudstones and minor sandstones of hemipelagic deep-marine environment. The Upper Cretaceous, which includes Arroyo Castorera, Río Rodríguez and Policarpo

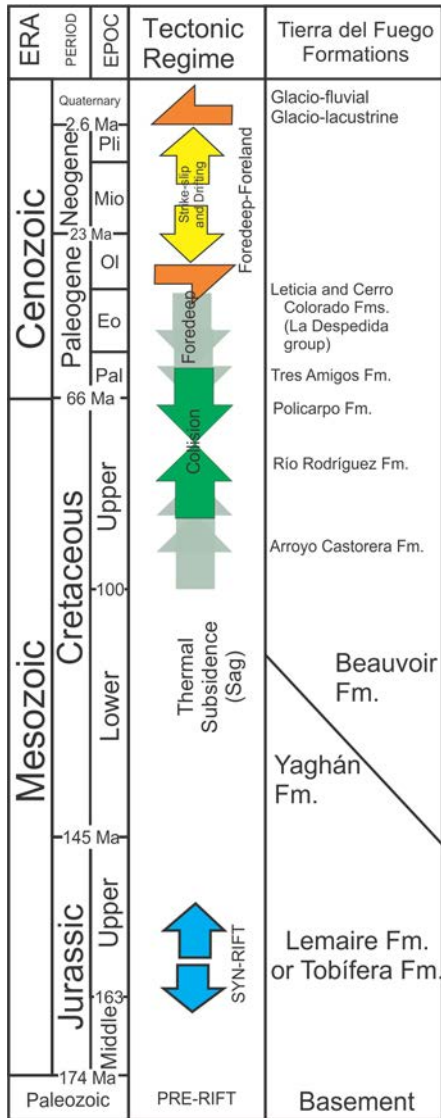


FIG. 3. Chrono-stratigraphic chart. Modified from Menichetti *et al.* (2008). Stratigraphy based on Olivero and Malumián (2008) and Martinioni *et al.* (2013).

formations, is mudstone-dominated, with an upward increase in coarse sand material and represents the transition to the Late Cretaceous Austral foreland basin evolution. This transition is interpreted as turbiditic deposits that were progressively accumulated in front of the rising Fuegian Andes (Martinioni *et al.*, 2013). The Paleocene Tres Amigos Formation (Cerro Apen Beds in Martinioni *et al.*, 2013) consists of conglomerates, sandstones and siltstones from fan delta deposits. The Leticia and Cerro Colorado

formations (both from Eocene of La Despedida Group) crops out in the northeast. These formations consist of mudstones and sandstones from a coastal and estuarine environment.

The outcrops at the margins of LY belong to the Late Cretaceous Policarpo Formation, the Paleocene Tres Amigos Formation and to widespread Quaternary sedimentary deposits (Fig. 4H). The Mesozoic unit corresponds to grey mudstones (Fig. 4A, C, D) and sandstones (Fig. 4B); the former often show compressive deformation (Fig. 4B, D) when involved in thrusts. Tres Amigos Formation outcrops are mostly sandstones (Fig. 4E, G) and coquinae (Fig. 4F) of fairly constant WNW-ESE strike sometimes displaced by thrusts (Fig. 4G).

A significant proportion of the area surrounding LY is dominated by Quaternary deposits, mostly of glacial origin. During the Late Pleistocene, glaciers spread from the cordillera Darwin ice sheet, and flowed to the east (Caldenius, 1932; Bujalesky *et al.*, 1997). During the Last Glacial Maximum, ca. 25,000 yr B.P. approximately 50 alpine-type glaciers flowed from the northern and southern sides of the Fagnano glacier (Coronato *et al.*, 2009; Rabassa *et al.*, 2011). Among these, two ice-tongues-Fuego and Ewan main lobes-flowed through the studied area (Fig. 2), as evidenced by frontal moraines along the valleys of Fuego and Ewan rivers. Many sequences of glacio-fluvial terraces are found through the river valley. In the Fuego river valley, three levels of terraces including lateral moraines, with thin gravel covers in the higher terraces; along the Ewan river valley and the eastern margin of Lago Chepelmut, several glaciofluvial terraces are located. The area situated between the Chepelmut and the Yehuín moraine is characterized by a landscape formed by hills and depressions as a consequence of the ice ablation, with remnants of paleolakes (Coronato *et al.*, 2008a, b).

3. Data acquisition

Between March-April 2014, 15 high-resolution single-channel seismic profiles were acquired with an acquisition system installed on a Zodiac boat, and consisting of a Boomer as a seismic source and a single-channel, 10 m long oil-filled streamer (Fig. 5). The seismic source is an electro-dynamic transducer UWAK mounted on a catamaran frame that suspends the plate at a constant depth of 40 cm to avoid potential turbulences on the lake surface during dragging. The

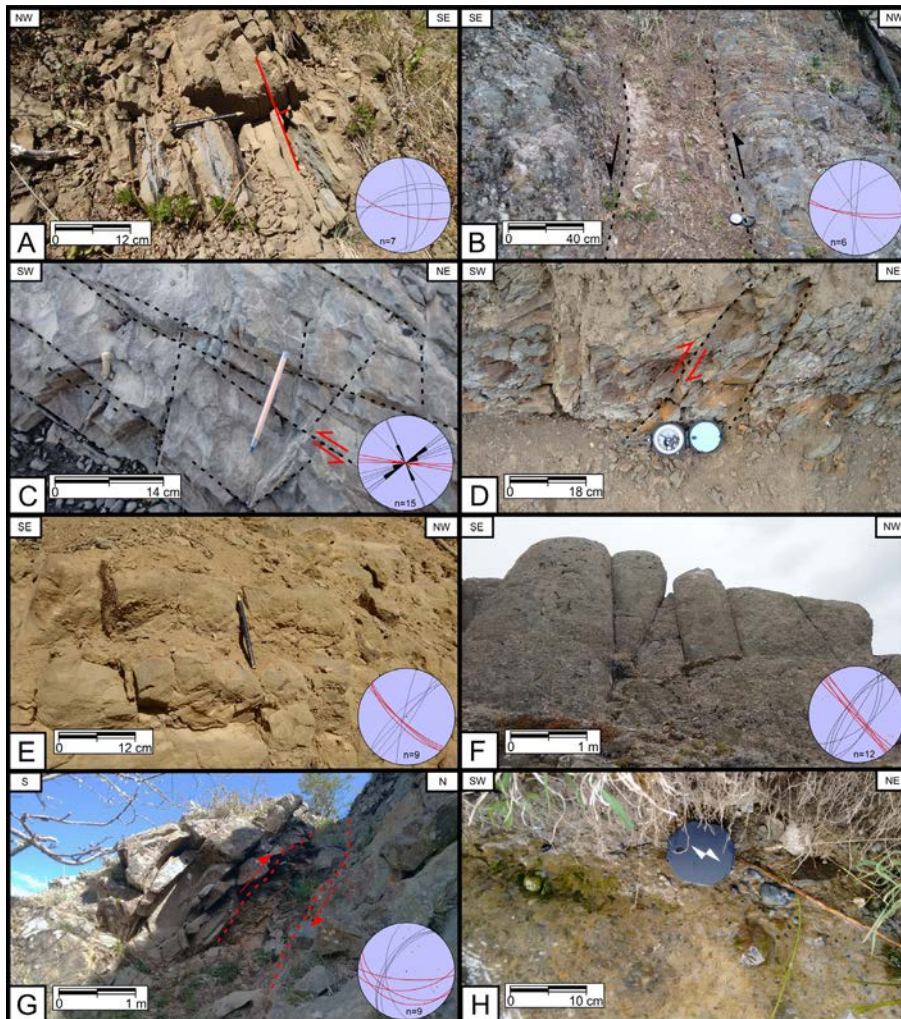


FIG. 4. Photographs and structural data in the lago Yehuín area. Lower hemisphere equal area plots of joints and faults (black lines) and bedding planes (red lines). Number (n) of measurements is also indicated. **A.** Outcrop of Policarpo Formation, of Campanian-Maastrichtian age, close to the road and near Estancia Ushuaia (NE view). The lithology consists of grey mudstones with incipient bedding affected by two joint systems; **B.** Outcrop of the sandstone member of the Policarpo Formation at cerro Cabras. The dashed lines limit a sub-vertical shear zone pertaining to the Cerro Cabras thrust; **C.** Grey mudstones of Policarpo Formation at the southeastern margin of Lago Yehuín with several joint systems, with cross cutting relations. The red arrows indicate the E-W slip of a sinistral fault that could be related with the transpressive left-lateral tectonic phase; **D.** Mudstone of Policarpo Formation in the SW area of Lago Yehuín affected by low angle compressive structures overprinted by subvertical faults; **E.** Outcrops of Tres Amigos Formation made of sandstones displaying parallel bedding; **F.** NW-SE view of Tres Amigos Formation outcrops in cerro Shenolsh exposing coquina affected by sub-vertical joints; **G.** Thrust in sandstones of Tres Amigos Formation near Estancia Los Cerros. The red dashed lines limit a thrust fault of W-E strike and north vergence; **H.** A conglomerate cropping out in the SW area of lago Yehuín, interpreted as of glacial origin.

UWAK accepts 300 Joule from a high voltage power supply of almost 2.5 kV and creates a pulse with good repeatability rate and a large spectrum between 400 Hz and 7,000 Hz (Donda *et al.*, 2008). The streamer is pre-amplified and composed of ten hydrophones

with a high sensitivity and bandwidth of 100-10,000 Hz that stacks signals without Normal Move Out (NMO) correction. The streamer active sections can be changed closing hydrophones according to the water depth; but in very shallow water, to avoid

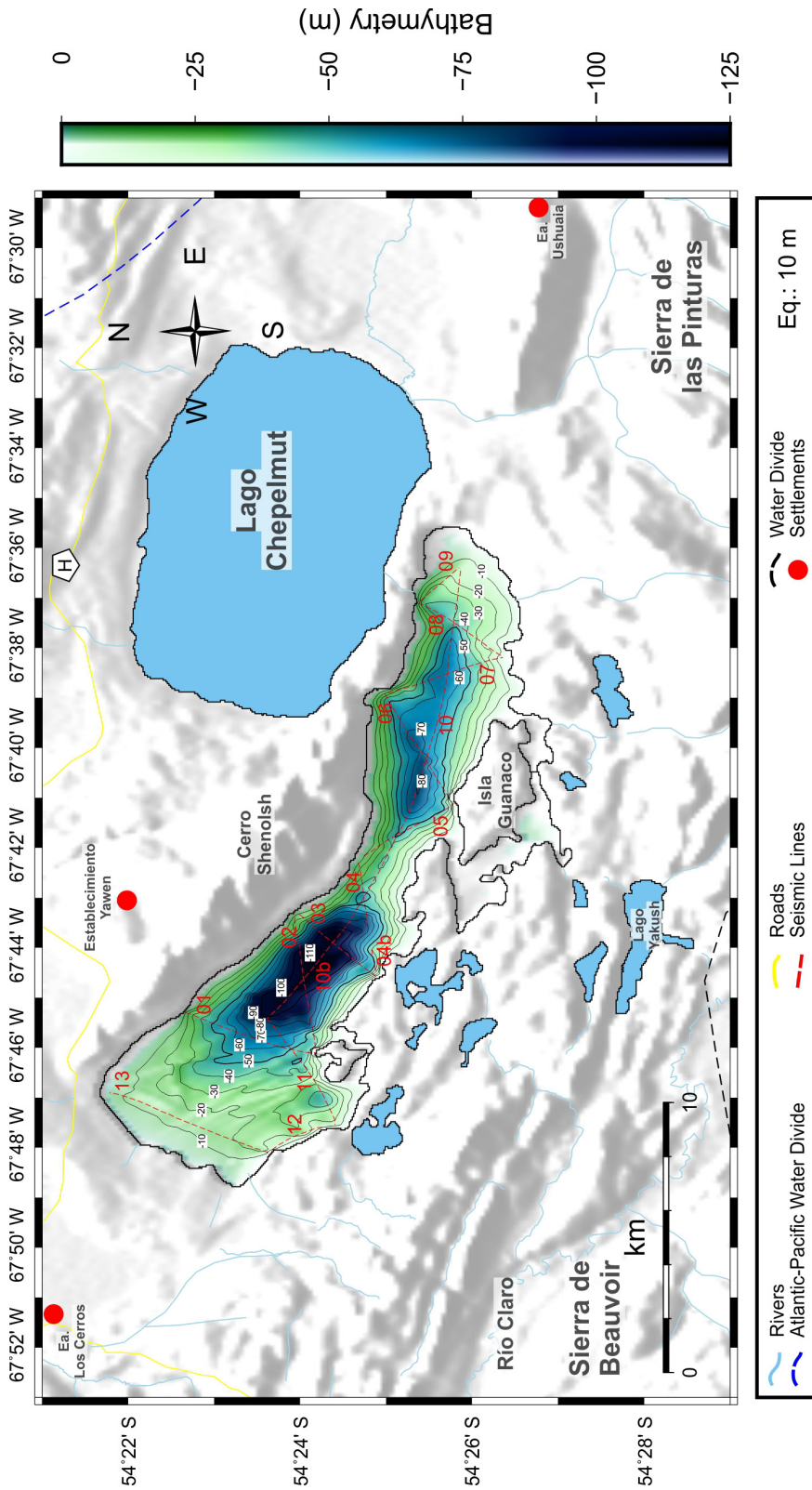


FIG. 5. Lago Yehuín area with the main geographic references and location of the acquired seismic lines (red lines within the lake; red numbers indicate the different lines in order of acquisition). The hydrographic network is also displayed and subdivided in two sectors (separated by a black dashed line): the drainage in the southern sector belongs to the Fagnano drainage basin; the drainage net in the northern sector -including lago Yehuín and Chepeimut- is strongly controlled by the morphostructure imposed by the NNW-verging Magallanes fold-and-thrust belt. The blue dashed line is the Atlantic/Pacific water divide. Also, the bathymetric map of lago Yehuín is displayed, highlighting the two sub-basins separated by a central high in the narrowest part of the lake. The lake shoreline is 43 m a.s.l. Contour lines are every 10 m.

destructive effects of signal stack without NMO, we collected seismic data with a parallel geometry (Baradello and Carcione, 2008). In this geometry, the streamer and the source are towed at a same distance from the boat (10 m in this survey). To prevent the destructive interferences between reflections and their multiple events from air/water, the streamer was kept floating at less than 10 cm below the lake surface. Seismic data, recorded in SEG Y format, had a time window length of 400 ms with a sampling rate of 50 μ s. All the acquired data have been D-GPS navigated. Along-track horizontal resolution of 1 trace every 1 m was achieved shooting at 0.5 s interval (at an average boat speed of 4 knots). After editing, to improve the signal/noise ratio of data we applied a time-variant filtering and spike deconvolution. The seismic records have been uploaded, displayed and interpreted using the Kingdom Suite® software package (version 8.3). To convert the two-way travel time of the high-resolution profiles to depth, a water sound velocity of 1,432 m/s was used, following Zanolla *et al.* (2011). The depth conversion has been done picking the lake floor horizon. For the lacustrine, fluvial and glacial sediments, a sound velocity of 1,600 m/s was assigned according to previous works performed in Lago Fagnano (Waldmann *et al.*, 2008, 2010a; Esteban *et al.*, 2014).

The maximum distance between adjacent seismic lines does not exceed 4 km of separation. The majority of the seismic lines have N-S or NE-SW directions; a single seismic line (tie line) was acquired along a WNW-ESE direction to intercept perpendicularly most of the other seismic profile (Fig. 5) to allow stratigraphic correlations. Grids were created using a Kriging method with cells spaced at 0.00115°. The spacing was adequate to obtain results with the minimum amount of grid artifacts. We use a forcing factor along the NW-SE direction considering the particular elongated geometry of Lago Yehuín. In order to remove incoherent data, minor editing was applied to these grids. Finally, the GMT software (Wessel and Smith, 1991) was then used to generate all the maps displayed in this work.

4. Bathymetry and seismic interpretation

4.1. Bathymetry of lago Yehuín

The high-resolution seismic profiles have been used to elaborate the bathymetric map of LY (Fig. 5). The lake basin is divided in two sub-basins, separated

by a shallow morphologic relief located in the center of the lake, where the basin presents the minimum width. These two sub-basins are named Eastern and Western sub-basins, respectively. The Western sub-basin has a length of 7.5 km and a maximum depth of 118 m (the lake shoreline is located at 43 m a.s.l.). This sub-basin is asymmetric, with a relatively gently western slope (2.6°) with respect to the slope at the eastern side (8.5°). The northern (15°) and southern (18°) margins have similar slopes, although the relief of the southern margin is more irregular in profile. The Eastern sub-basin has a length of 7.2 km and a maximum depth of 80 m. This sub-basin displays an asymmetric profile, quite gentle at the eastern margin (2.3°) and more abrupt at the western margin (5°). The northern margin (8°) has a more abrupt slope than the southern margin (6°). As in the Western sub-basin, the relief of the southern margin is rougher than the northern margin.

The presence of two small islands in the center and eastern part of the lake (one island is known as “La Piedra”, the other island is unnamed) represent significant elevations in the morphology of LY and of the central high, reaching heights of more than 20 m above the lake water level.

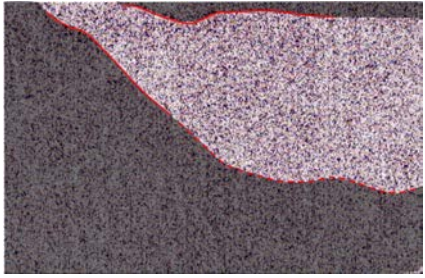
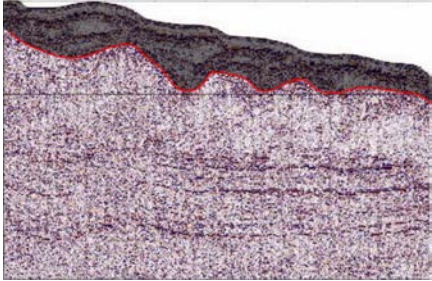
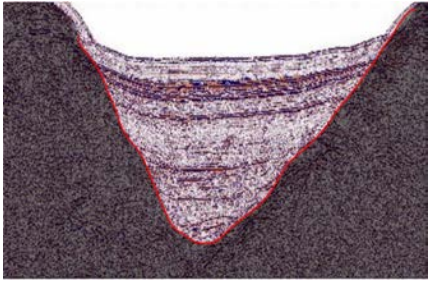
4.2. Seismic interpretation

Three seismic units have been individuated in the seismic record acquired within LY (Table 1; see Pugin *et al.*, 1999; Fernández *et al.*, 2017). These units were defined as parts of the seismic sections based on their geometric patterns, architecture and stratigraphic relationships. Each seismic unit highlight a specific seismic facies (SF) which were identified based on concepts of depositional systems and seismic sequence stratigraphy (Mitchum *et al.*, 1977; Table 2). The three seismic units are:

- Lower Unit-LU (SF I).
- Intermediate Unit-IU (SF II, SF III, SF IV, SF V and SF VI).
- Upper Unit-UU (SF VII, SF VIII, SF IX).

All the seismic units rest on a recognizable acoustic basement whose top is generally defined by a continuous and high-amplitude reflector, H0 (Table 3). Deepest depressions defined by the stepped geometry of H0, host the Lower Unit which top corresponds to a medium to low-amplitude and discontinuous reflector, H1, interpreted as an angular to erosive unconformity. Resting either above H0 or H1, the

TABLE 1. SUMMARY OF THE MAIN CHARACTERISTIC OF THE SEISMIC UNITS.

Seismostratigraphic Unit	Short Term	Seismic Facies	Main Characteristics	Sample View
Mass-flow deposits- Lower Unit	LU	SF I	Weak and discontinuous reflectors of medium amplitude at base and top. Chaotic structure and transparency zones. Small deposits.	
Glacial and Glaciolacustrine deposits-Intermediate Unit	IU	SF II, SF III, SF IV, SF V, SF VI	High amplitude reflectors at base and top. Strong parallel reflectors; sometimes chaotic. Some zones shows transparency. Mainly founded in the western sub-basin.	
Lacustrine deposits- Upper Unit	UU	SF VII, SF VIII, SF IX	Strong and continuous reflectors at base and top. Internal structure with layers and continuous reflectors, sometimes with a periodic alternation between strong and weak reflectors. Located in both western and eastern sub-basins.	

Intermediate Unit is capped by a high amplitude, sometimes discontinuous and strong reflector, H2, displaying small depressions. Given the irregularity of H2 and the contact with the overlying reflectors, this surface is interpreted as an erosive unconformity. The acoustic basement (SF0) is characterized by highly discontinuous, chaotic reflectors with some transparent intervals. Based on the geology of the area and the outcrops observed in the lake shoreline (Figs. 2, 4) the basement likely corresponds to Upper Cretaceous-Paleocene rocks pertaining to the Policarpo and Tres Amigos formations.

Detailed observation of offsets and displacements within the reflectors allowed to identify several discontinuities within the acoustic basement. Two groups were recognized, the most remarkable occurs

as medium to high angle planes which are interpreted as normal faults; the second group corresponds to low angle planes which are overprinted and displaced by high angle surfaces. On the basis of their fairly constant south gentle dip, this older group is correlated to the thrust faults mapped onland (Figs. 2, 6, 7). The steeply dipping to vertical basement-involved faults bound small grabens and constitute an overall negative flower cross-sectional pattern (Fig. 7).

4.2.1. Lower Unit

The oldest unit is restricted to the deepest depressions of both sub-basins (Fig. 8A). Their maximum thickness is approximately 36 m in the Western sub-basin. The fabric is mainly chaotic with some intervals of parallel reflectors, which are north-dipping (Fig. 9A).

TABLE 2. SUMMARY OF THE CHARACTERISTIC OF THE SEISMIC FACIES.

Seismic Facies	Color	Main Characteristics	Facies Zoom
Acoustic basement	Without color	Highly discontinuous and chaotic reflectors, sometimes with transparency.	Figure 8
SF I	Purple	 Oldest. Weak and discontinuous top and base reflectors. Chaotic internal structure and zones with transparency. Some sectors have a north-dipping layered structure.	Figure 8A
SF II	Yellow	 Base and top with strong reflectors of high amplitude. The top reflector can be interpreted sometimes as an erosive surface. Thick facies with a chaotic internal structure. Extended deposits, mainly in the western sub-basin.	Figure 8B, D
SF III	Brown	 High intensity top and base reflectors. It is composed by layered, strong to medium internal reflectors.	Figure 8C, D, E
SF IV	Orange	 Strong to medium intensity, high amplitude base and top reflectors. Chaotic internal structure, sometimes weak-layered. Terrace morphology.	Figure 8F
SF V	Magenta	 Strong, discontinuous, high-amplitude base reflectors; low-amplitude reflectors against the overlying seismic units. Chaotic internal structure. Located in the eastern sub-basin, in a shallow zone.	Figure 8G
SF VI	Gray	 Disturbed facies, located in slopes and near the breaks. Medium-strong top and base reflectors. Transparency. Thin facies.	Figure 8H
SF VII	Cyan	 Thick unit that fills the topographic depressions. Base and top reflector are continuous and strong; internal structure composed by layered and continuous reflectors. Periodic alternation of strong and weak reflectors.	Figure 8I, J, L
SF VIII	Green	 Thin facies. Strong and continuous top and base reflectors. Present in both sub-basins. Twelve continuous reflectors.	Figure 8K, L, M
SF IX	Red	 Uppermost facies. Thin and youngest facies. Weak, continuous and parallel reflectors located in both sub-basins. Strong top and base reflector.	Figure 8L, M

SFI. The basal facies SF I (Fig. 9A) is bounded at the base and top by weak and discontinuous reflectors of medium amplitude; it has a chaotic internal structure with some transparent intervals and shows onlap terminations against the basement top. This facies is restricted to the deepest depocenters, with a maximum preserved thickness of 0.024 TWT seconds (corresponding to 36 m) in the Western sub-basin. SF I can also be recognized in a small depocenter between seismic lines 07 and 08 in the Eastern sub-basin (Fig. 6) displaying an internal structure of north-dipping, weak reflectors.

4.2.2. Intermediate Unit

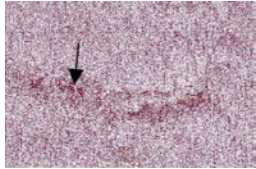
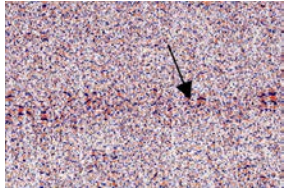
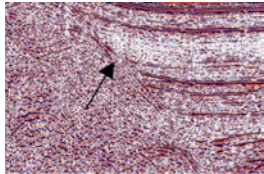
The entire collection of seismic facies which compose this unit makes it the thickest (Fig. 8B). The acoustic fabric is either chaotic or vaguely layered (Fig. 9G), whereas in cross sections reflectors display a folded pattern (Fig. 9D). Major accumulation is located in the Western sub-basin and exceeds 120 m in thickness, near the western margin. Also, the distri-

bution of the isopachs shows a major deposition trend along a NW-SE axis, which correlates with the basement morphology (Fig. 10). Three mounds thicker than 60 m are located near seismic lines 2, 3 and 4 (Fig. 8B). Five seismic facies are included in this unit:

SF II. Described for the Western sub-basin, facies SF II (Fig. 9B) is bounded at the base and top by strong reflectors of high amplitude and comprises a thick package (≤ 0.07 TWT s, 100 m). It is characterized by a chaotic seismic fabric, with geometries of crested ridges less than 100 m high and 200-400 m wide (Figs. 6, 7).

SF III. Facies SF III (Fig. 9C) comprises a thick package of 0.06 TWT s. It displays a layered structure with parallel, strong to medium reflectors. Its upper reflector shows some diffractions mainly in the Western sub-basin (Fig. 6). Some irregular discontinuities are observed within this facies; against these unconformities. The irregular top surface defines small depocenters. This can be interpreted

TABLE 3. SUMMARY OF THE THREE HORIZONS THAT BOUND THE SEISMOSTRATIGRAPHIC UNITS.

Horizon	Short term	Bounds	Main Characteristics	Sample View
Horizon 0	H0	Basement top-Lower Unit base	Deepest, continuous and high-amplitude reflectors.	
Horizon 1	H1	Lower Unit top-Intermediate Unit base	Medium to low amplitude, discontinuous reflectors.	
Horizon 2	H2	Intermediate Unit top-Upper Unit base	High amplitude, discontinuous and strong reflectors. Interpreted as an erosive unconformity.	

as a depositional landform or, in some sectors, as an erosive unconformity.

SF IV. Strong to medium intensity and high amplitude reflectors enclose this facies (Fig. 9F) which shows a chaotic internal structure, with some weakly-layered sectors. This facies is only observed in the Eastern sub-basin and displays a distinct morphology characterized by several terraced surfaces (Fig. 6).

SF V. Asymmetrical ridges located in the eastern margin of LY, thicker than 0.050 TWT s (about 75 m) (Figs. 9G, 6) and a few kilometers wide, with strong, discontinuous, high-amplitude base reflectors against of the acoustic basement and strong, continuous, low-amplitude reflectors against of the overlying seismic units. It has a smooth slope, chaotic internal structure with some intervals of sub-parallel, low-amplitude, discontinuous reflectors. This unit would be equivalent to SF II of the Western sub-basin.

SF VI. Disturbed facies (Fig. 9H) located near slope-breaks identified only in the Eastern sub-basin (Fig. 6), with limited thickness (0.008 TWT s). SF VI has a medium-strong top and base reflectors; the acoustic fabric is characterized by discontinuous reflectors and some transparency.

4.2.3. Upper Unit

This unit is characterized mainly by the presence of layered and continuous reflectors with a draped distribution, filling the depressions. The isopach map of the Upper Unit (Fig. 8C) shows isolated packages of a variable thickness, with the thickest ones located in the center of the Western sub-basin, reaching almost 25 m. In the Eastern sub-basin, the thickness is reduced to about 10 m.

The distribution of the total sedimentary infilling of the YB (Fig. 8D) shows a preferential accumulation along a NW-SE axis. The maximum sediment thickness in the entire lake is 140 m near the western margin. Three seismic facies are included in this unit:

SF VII. A thick unit (Fig. 9I, J) that fills the variable topography formed by the underlying seismic facies (acoustic basement, SF II, SF III, SF IV and SF VI), reaches a maximum thickness of almost 0.020 TWT s (30 m). Its distribution involves both the Western and Eastern sub-basins (Figs. 6, 7). The base and top is characterized by strong and continuous reflectors; its internal structure is composed by layered and continuous reflectors with a periodic alternation of strong and weak reflectors.

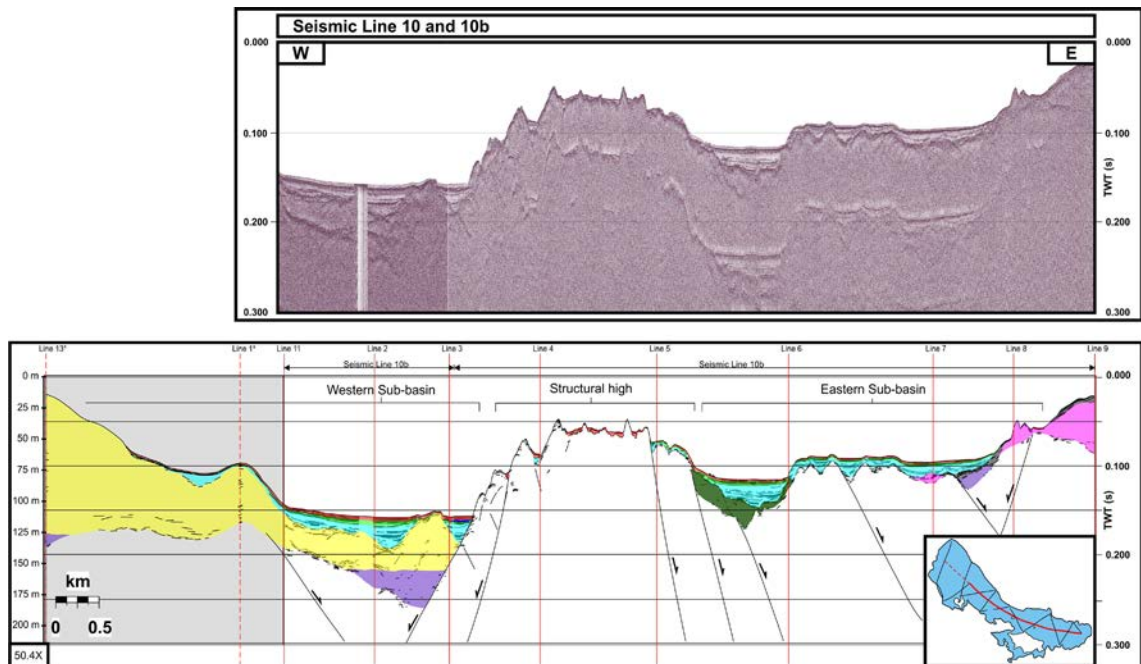


FIG. 6. Above, uninterpreted NW-SE high resolution single-channel seismic profiles 10 and 10b. Below, interpreted sketch; depth is given both in seconds of two-way traveltime (TWT) and converted to sub-lake level depth (m) based on a P-wave velocity of 1,430 m/s for water and 1,600 m/s for the sedimentary section. Vertical exaggeration is shown in the lower left side of the interpreted section. Vertical dashed red lines indicate crossing seismic profiles (location shown in figure 5). The black lines are interpreted normal faults. The western sector, grey shadowed, is a composite section resulting from interpolating seismic lines 11, 12 and 13 and using the bathymetric map. The sketch displays the distribution, geometry and internal seismic reflectors pattern of the ten recognized seismic facies within the entire Lago Yehuín basin. The seismic facies (SF) are displayed in different colors: purple for SF I; yellow for SF II; brown for SF III; dark green for SF IV; magenta for SF V; gray for SF VI; cyan for SF VII; green for SF VIII; red for SF IX; the acoustic basement is in white color.

SF VIII. A thin unit (~ 0.002 TWT s, 3 m) that overlies SF VII in both sub-basins (Figs. 6, 7), bounded by strong and continuous reflectors (Fig. 9K). Within SFVIII twelve strong, continuous and parallel reflectors are recognized; locally a small package of a few chaotic and transparent reflectors is enclosed within SF VIII (Fig. 9I).

SF IX. It represents the uppermost, thinnest (≤ 0.002 TWT s, ≤ 3 m) and youngest seismic facies (Fig. 9M) which drapes the entire lake floor (Fig. 6). Strong top and base reflectors enclose an internal fabric composed by weak, continuous and parallel reflectors.

4.3. Basement map

The topography of the basement top (Fig. 10) shows two main depressions separated by a structural high in the center of the lake, which mimics fairly well the lake bathymetry (Fig. 5). At the west and

east of this raised zone, the depth of the basement increases progressively to reach a maximum in the Western and Eastern sub-basins. In the former, the depth reaches a maximum of 160 m below lake level, while in the Eastern sub-basin the maximum depth is reduced to 100 m. The morphology of the acoustic basement, in the western side, is a trench-like depression of WNW-ESE strike bounded by high-or-intermediate angle normal parallel faults (Fig. 7) that produce a stepped basement surface.

5. Discussion

5.1. Geological interpretation of the seismic units

5.1.1. Lower Unit

The acoustic configuration of this unit, mainly chaotic with intervals of parallel, north-dipping reflectors limiting transparent bodies corresponds

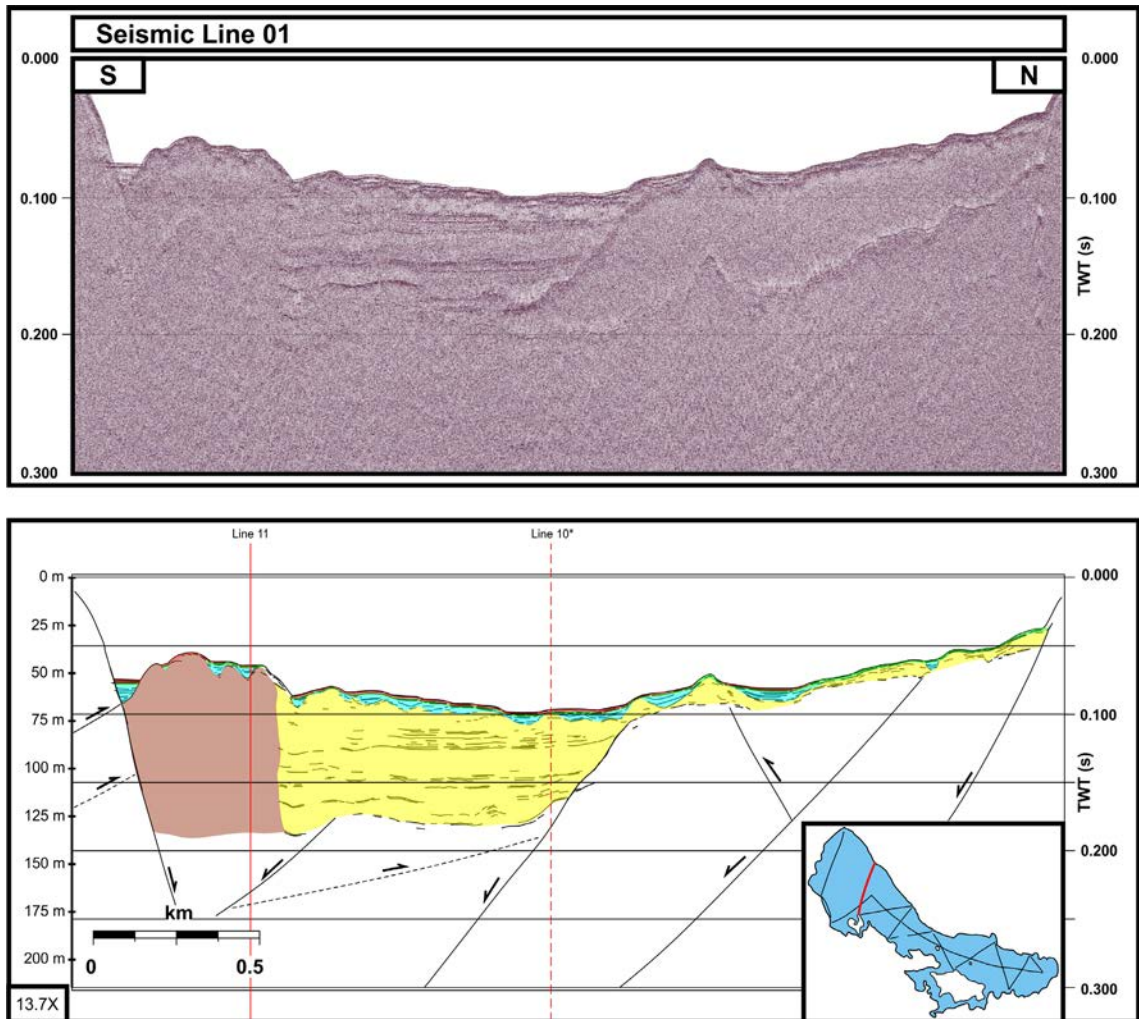


FIG. 7. Above, uninterpreted N-S high-resolution single-channel seismic line 01, located in the Western sub-basin. Below, interpreted sketch of the section; depth is given both in seconds of two-way traveltime (TWT) and converted to sub-lake level depth (m). Color code of seismic facies is the same as in figure 6. An irregular topography is observed. Vertical exaggeration is shown in the lower left side of the interpreted section. Vertical red lines indicate crossing seismic profiles 10* (dashed) and 11 (solid); locations are shown in figure 5. The acoustic basement hosts a large depocenter in the central zone. Two sets of faults were recognized: older thrust faults overprinted by normal faults displaying an upward branching pattern. SF III (brown) presents a chaotic seismic pattern and it is founded in a marginal location; SF III, with layered fabric, is located at the north of SF II (yellow). SF VII, SF VIII, SF IX are located over these glacial deposits (seismic unit IU).

to wedged deposits, and interpreted as mass-flow deposits (Waldmann *et al.*, 2010b). This architecture, with the divergent reflector pattern (Fig. 9H) has been previously recognized in similar environments such as the Alpine lakes system (*i.e.*, Chapron *et al.*, 1996; Schnellmann *et al.*, 2002). Based on the lack of observable deformation of the sedimentary cover by faulting, this unit is considered post tectonic.

5.1.2. Intermediate Unit

Seismic facies that compose this unit (SF II, SF III, SF IV, SF V and SF VI) are similar to others that have been interpreted elsewhere as till deposits (Eyles *et al.*, 2000; Waldmann *et al.*, 2008, 2010a, 2010b; Pinson *et al.*, 2013). These characteristics include groups of discontinuous to chaotic reflectors of high to low amplitude, interpreted as coarse grain sediment of glacial diamicton (Pinson *et al.*, 2013).

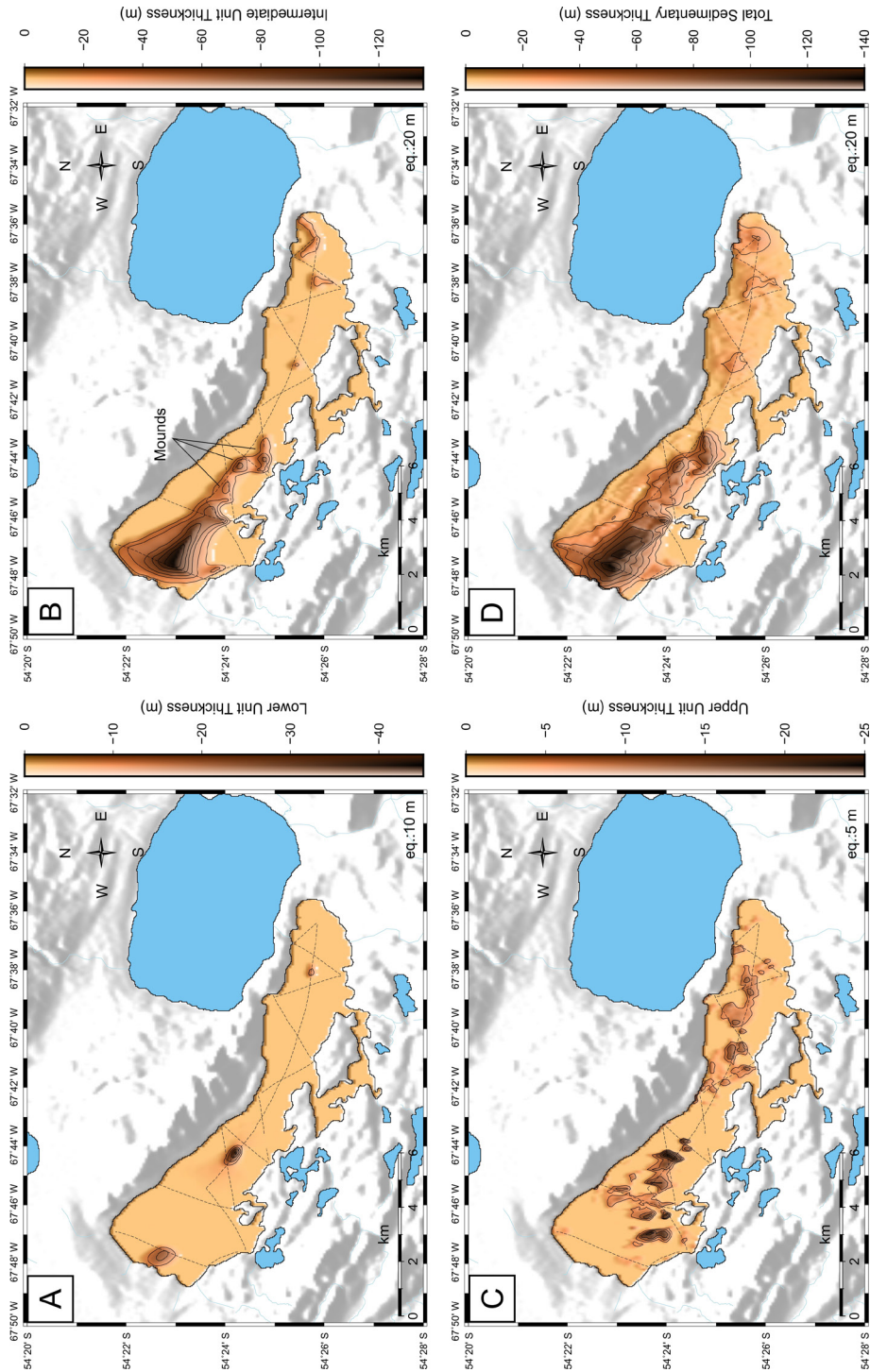


FIG. 8. Maps of sedimentary thickness for the different seismic units. **A.** Sedimentary thickness of the Lower Unit. The distribution is irregular, with thickest deposits mostly concentrated in the deepest sectors of the basement, forming three depocenters: two at the Western sub-basin and one at the Eastern sub-basin. **B.** Sedimentary thickness of the Intermediate Unit. The thickest sedimentary package is located in the Western sub-basin (~120 m). The deposit fills a trench like depression within the basement, which widens westwards. In the Eastern sub-basin, the deposits are scarce, concentrated mainly near the eastern margin; **C.** Sedimentary thickness of the Upper Unit. The distribution of this unit is highly irregular, forming isolated depocenters located within small depressions of the top of the intermediate unit. It is important to remark that some isolated depocenters in the Western sub-basin are located where there is a gap in the seismic data; **D.** Total sedimentary thickness. The major thickness is located in the Western sub-basin and corresponds mainly to the IU seismic unit.

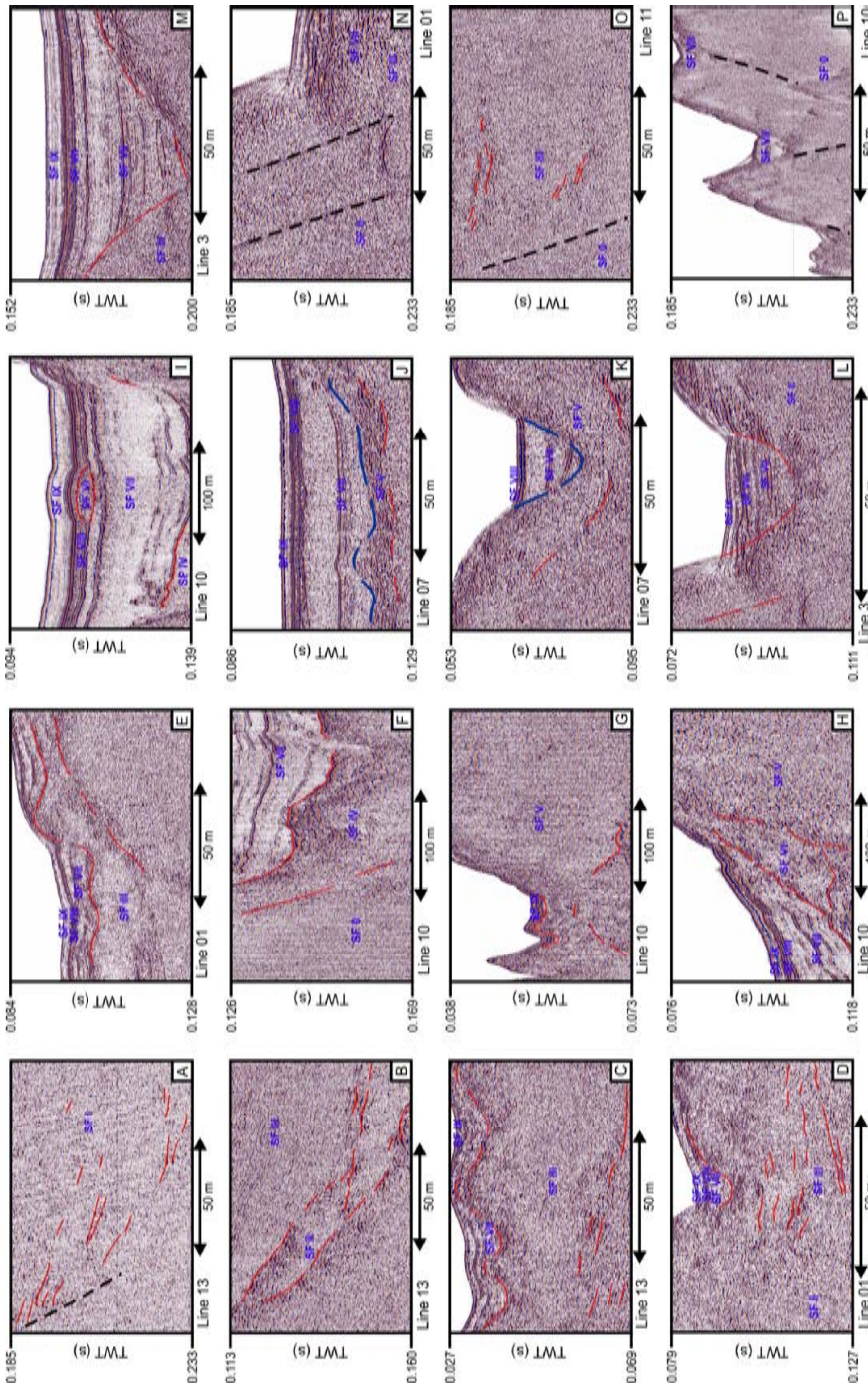


FIG. 9. Selected sectors of the seismic profiles showing the different seismic facies. **A**, Deposits of the LU (SF I) showing the north-dipping reflectors; **B**, An interpreted lateral moraine (SF II), resulting from ice retreat; **C**, Upper part of the IU deposits (SF III), underlying the UU (SF VII-SF IX); **D**, Detail of SF II showing the chaotic internal structure at the left side. At the right side, a view of SF III showing the layered internal structure; **E**, Deposits of SF VII, VIII and IX over small depressions on SF II; **F**, Detail of SF IV in the eastern sub-basin (red lines separates seismic facies); **G**, Detail of SF V near the eastern margin of Lago Yehuín showing the chaotic internal arrangement; **H**, Deposits of SF VI in the slope break of the deposits of SF V; **I**, A small deposit of SF V-outlined in red- between SF VII and SF VIII. This can be the result of a mass movement triggered by gravity; **J**, UU over a thin deposit of the IU (bounded with a blue line); **K**, Another view of the UU over the IU; **L**, Deposits of SF VII, VIII and IX located in a small depression on SF II top; **M**, Thickest deposit of the UU showing details of the reflector configuration of SF VII, VIII and IX; **N**, Two small normal faults that affect the basement in the Western sub-basin. These faults bound SF 0 (acoustic basement); **O**, A normal fault affecting the basement in the Western sub-basin; **P**, A view of the central high in the seismic line 10 showing some normal faults affecting the SF 0.

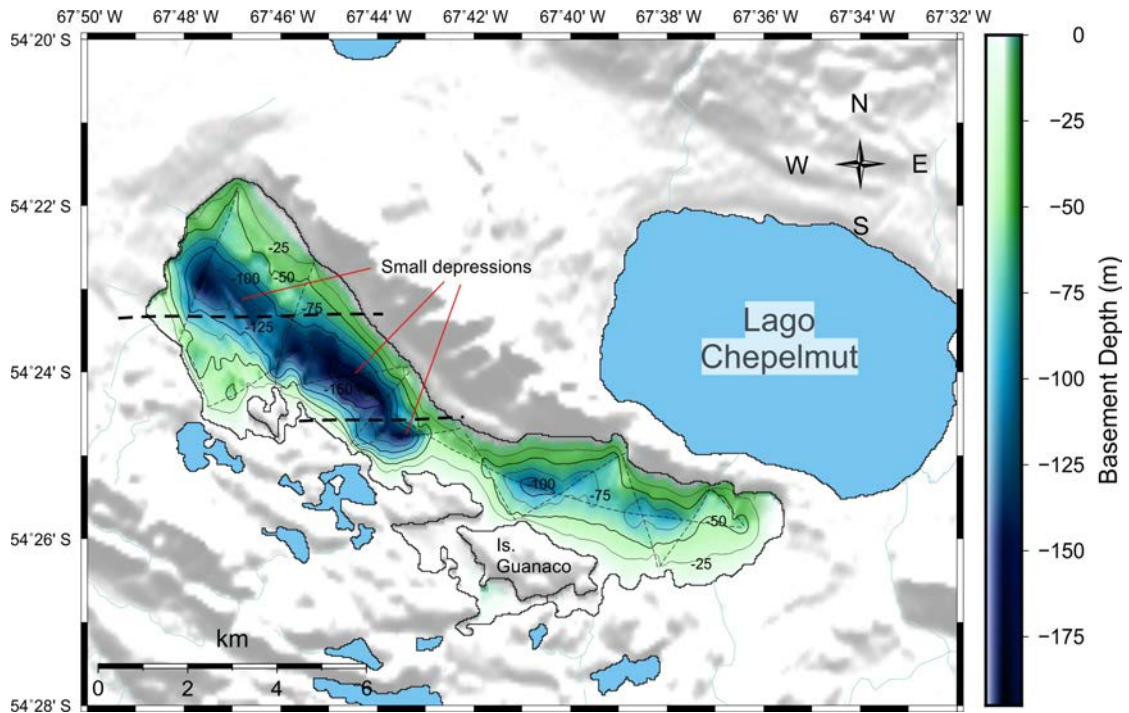


FIG. 10. Topographic map of interpreted basement beneath Lago Yehuin with 25 m contour interval. The separation of the basin into two sub-basins is still recognizable. In the Western sub-basin, the basement forms an elongated depression; the form is less defined in the Eastern sub-basin. Seismic lines 10 and 10b (Fig. 6) displays this compartment. Segmented lines represent the seismic lines.

Moreover, the crested morphology of SF II, SF V and their distribution forming ridges (of roughly NE-SW strike in the Western sub-basin and NW-SE in the Eastern sub-basin) are interpreted as moraines, formed at the ice-margin by a temporary advance and/or still-stand of the glacier front (Fig. 6).

The lowermost seismic facies of this unit (SF II in the Western sub-basin and SF V in the Eastern sub-basin) is represented by the three mounds recognized in the figure 8B. These are composed by a mainly chaotic configuration of the reflectors and sometimes with an incipient layering, which can be ascribed to a complex till landform (Pinson *et al.*, 2013). These deposits can be interpreted as moraine deposits based on the similarity (mainly the ridge-shape) with features described by other authors (*i.e.*, Pugin *et al.*, 1999; Fernández *et al.*, 2017). The distribution of the seismic lines across the lake allows to recognize this seismic unit and their morphology in different parts of the LY (Fig. 8B). These moraine arcs could be deposited during the general retreat of the glaciers in the region. The regression of the Fuego glacier lobe went through

the Fuego river valley and has cut across the Western sub-basin of LY. During this regression, the ice lobe deposited several frontal moraines along the entire river valley (Coronato *et al.*, 2008a).

SF III, with a slightly layered internal structure (Fig. 9C), can be interpreted with a more remarkable influence of lacustrine sedimentation processes, *i.e.*, an outwash plain. Its location, laterally near SF II, may suggest an interaction with glacial sedimentation processes.

SF IV, a facies with terrace morphology, is interpreted as due to fluvial action (Fig. 9F). As an example, similar facies has been recognized in Lake Malawi in East Africa (Scholz *et al.*, 1998; Lyons *et al.*, 2011), Lake Baikal and Lake Tanganyika (Scholz *et al.*, 1998) and southern Ontario (Pugin *et al.*, 1999). This type of seismic facies generally corresponds to channel valleys with their sedimentary infill and laterally-located terraces. Similar glacio-fluvial structures observed near the central hilly area of Lago Fagnano could correspond to proglacial delta forms (Bujalesky *et al.*, 1997), deposited after the retreat of the Fagnano palaeoglacier.

SF VI, the very restricted wedges of chaotic to transparent facies located on slope breaks (Fig. 9G, H), are interpreted as deposits likely produced by mass wasting events. This architecture has been already recognized in other similar glacial environments such as Alpine lake systems (Chapron *et al.*, 1996; Schnellmann *et al.*, 2002; Strasser and Anselmetti, 2008).

5.1.3. Upper Unit

The seismic facies that compose this unit (VII, VIII, IX) show a configuration defined by abundant layered and continuous reflectors. Comparison with other studies (*i.e.*, Waldmann *et al.*, 2010a) suggests that this configuration may represent lacustrine sedimentation. The high-amplitude reflections may represent fining upward sequences of turbidites or

small slides, mainly composed by coarse-grained (high-impedance) bases of debris flows and intercalated with clays and silts (Waldmann *et al.*, 2008). Correlations with sediment cores made by different studies commonly assign this acoustic type to inter-layering of fine-grained sediments from a lacustrine setting, where the facies are usually interpreted as a lake stage mud drape from an uniform suspension (*i.e.*, Waldmann *et al.*, 2008; Pinson *et al.*, 2013).

5.2. Areal lineament pattern and structure of lago Yehuín basin

A regional left-lateral, strike-slip tectonic regime was interpreted through the analysis of fault planes and their associated lineaments in the area of the

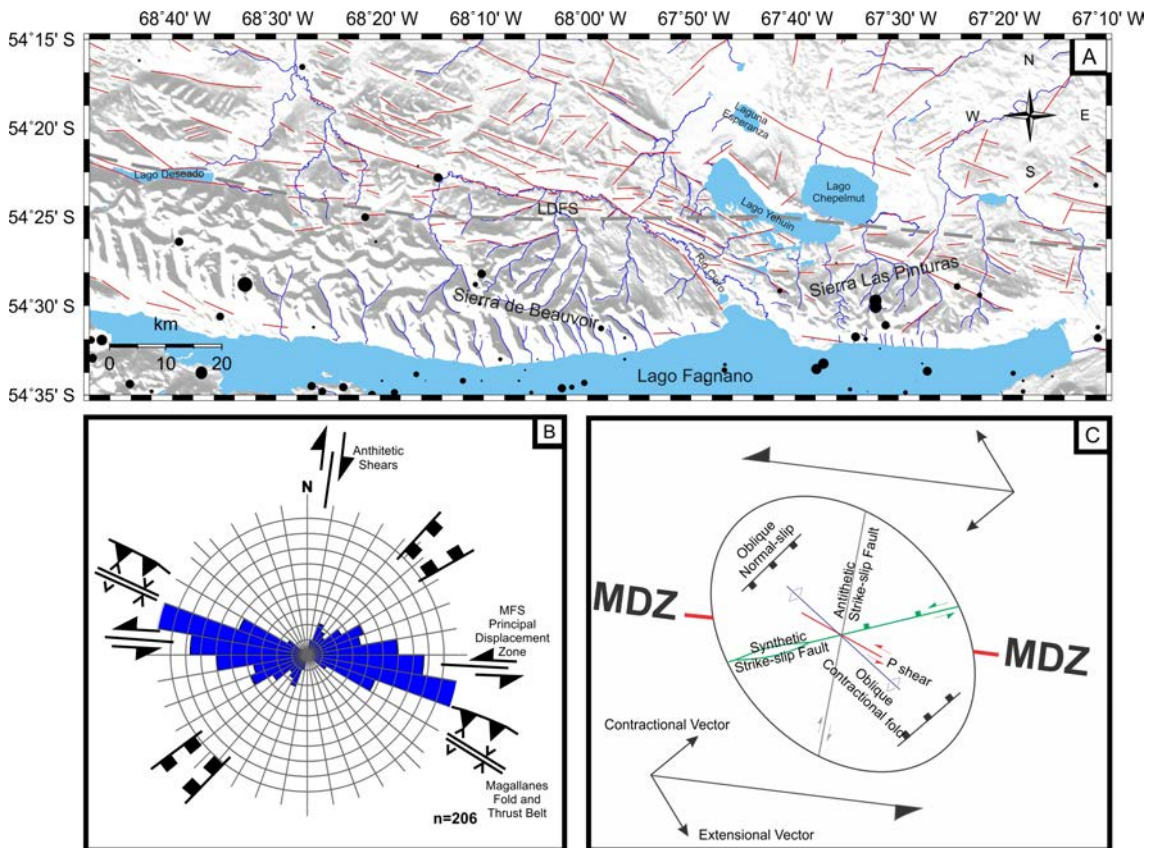


FIG. 11. A. Main structural lineaments from ASTER and SRTM images, in the area north of lago Fagnano, central Tierra del Fuego; black circles represent the hypocenter of shallow seismic events (between 0-30 km depth); the blue lines are the hydrography of the area; grey dashed line mark the position of the inferred Lago Deseado Fault System; the red lines are the identified lineaments; B. Rose diagram summarizing the azimuth and length distribution of the identified lineaments. Also, four lineament trends are shown around the rose displaying the interpreted tectonic significance from Lodolo *et al.* (2003); C. Riedel shear model for the area; MDZ: Main deformation zone.

external Magallanes fold-and-thrust belt (Klepeis, 1994a, b; Menichetti *et al.*, 2008; Torres-Carbonell *et al.*, 2008b). From a wide set of photo-interpreted lineaments derived from ASTER and SRTM images of the area north of Lago Fagnano (Fig. 11A), a correlation between groups of major trends with the structural geology can be established. The constructed rose diagram (Fig. 11B) has revealed the presence of a dominant trend with WNW-ESE (N100-110° E) strike, a main secondary trend oriented roughly W-E (N90-100° E) and subordinated trends spanning between N50° E to N120° E. A less significant trend is also recorded within the NE quadrant (N20-50° E). The rose diagram shows four main trends of lineaments identified in the eastern isla Grande de Tierra del Fuego with their interpreted tectonic significance (Lodolo *et al.*, 2003; Menichetti *et al.*, 2008). The lineament trends interpreted in our work matches fairly well with two of these: the Principal Displacement Zone of the Magallanes-Fagnano Fault System and the Magallanes fold-and-thrust belt. The overall distribution of these lineaments with respect to the general strike of the LDFS is quite consistent with a Riedel fracture model for a left-lateral shear system broadly oriented E-W (Fig. 11C). The ESE-WNW trend is associated with the deformation system of the Magallanes fold-and-thrust belt, which is particularly impressive in this area north of Lago Fagnano; some morphological depressions associated with strike-slip faults contribute to this trend. The NE-SW trend is distributed in the whole area, but is particularly evident to the north-northeast of Yehuin and Chepelmut lakes, where NE-SW trending discontinuities dissect older structural lineaments. Moreover, the hydrographic net significantly contributes to this trend (Fig. 11A). Widespread Neogene extensional reactivation of ancient Jurassic NE-SW transfer faults related to strike-slip tectonics was interpreted for the external FFTB (Ghigliione *et al.*, 2013). The orientation of the extensional structures in the Riedel shear model (Fig. 11C) matches fairly well with these reactivated extensional Jurassic faults.

The present-day tectonics in the area was analyzed by recent GPS studies along the Magallanes-Fagnano Fault System which indicates that the principal strain components define two deformation styles: a zone with predominant shortening of the crust to the west, and significant stretching on the east (Mendoza *et al.*, 2011). NW-SE extensional components and a subordinate contraction component with a SW-NE

trend have been reported for the LY area (Mendoza *et al.*, 2011, 2015). Therefore, LY basin is located within a regional framework dominated by transtensional, left-lateral deformation, and in particular within the deformation zone of LDFS (Fig. 1). Strike-slip basins are commonly classified by the structural setting of the strike-slip faults. The scheme proposed by Allen and Allen (2005) groups the basins in four main types. The term “pull-apart basins” are used to describe basins formed in local transtensional settings (Ingersoll and Busby, 1995). In the general setting of the Magallanes-Fagnano fault system and the Lago Deseado fault, the LY basin can be classified as a pull-apart basin.

Structures related both to the compressive stage and to the wrench tectonics have been interpreted from the analysis of the seismic records (Fig. 12). The strike of the thrust faults was defined by correlation with outcrops (Fig. 2), whereas the dominant NW-SE strike of extensional faults was determined by correlating the 15 seismic lines available in this work (Fig. 5). The negative flower pattern displayed by normal faults (Figs. 6, 7) in NE-SW and NW-SE sections support an overall left lateral kinematics. The strike of the faults controlling the central structural high, in turn, has been determined by correlation with the structures recognized in Cerro Shenolsh outcrops (Fig. 4E, F). In this context, the Cerro Shenolsh may be considered as the northern continuation of the central high within the LY (Fig. 12).

5.3. Paleogene compressional tectonics

Within the external FFTB, compressional deformation and emplacement of thrust sheets continued from the Ypresian to the Early Miocene (~56 to ~20-16 Ma) and was coeval with sedimentation in the foreland basin (Malumián and Olivero, 2006; Olivero and Malumián, 2008; Torres-Carbonell *et al.*, 2014). At about ~56 Myr, the front of the FFTB was located nearly the southwestern margin of the present LY (Fig. 13A); Policarpo and Tres Amigos formations were then involved in thrust sheets; out-of-sequence thrusts were later developed in the eastern area of LY (Torres-Carbonell *et al.*, 2014; Torres-Carbonell and Dimieri, 2013; Torres-Carbonell *et al.*, 2011; Olivero y Malumián, 2008) (Figs. 2, 12). A subsequent compressive phase in the external Fuegian FFTB was dated as Oligocene to Early Miocene (Torres-Carbonell *et al.*, 2013). In the Fuegian Atlantic margin, the last thrusts are unconformably overlain

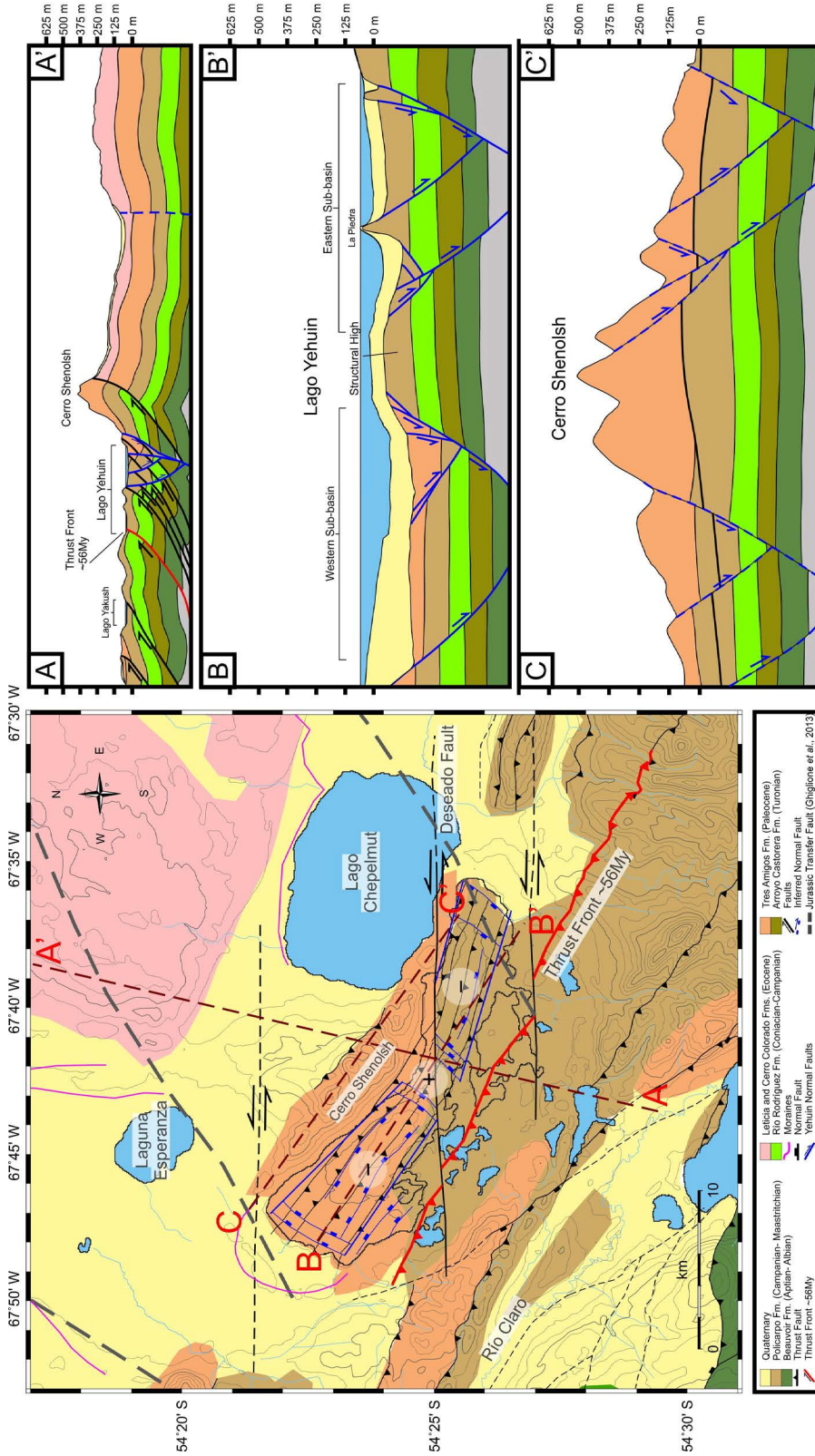


FIG. 12. Interpreted structures in lago Yehuín basin. The fault arrangement resulted from the correlation and integration of the newly acquired 15 seismic sections and onland data. The thick red line shows the location of the thrust front 56 Myr ago (Torres-Carbonell and Dimieri, 2013). The + and - symbols indicate the topographic relation of the basement between the structural high and the two sub-basins. The dark brown dashed lines show the location of geological sections; ENE trending, thick black dashed lines correspond to interpreted Jurassic transfer faults reactivated by Neogene tectonics (Ghiglione *et al.*, 2013). Moraine arcs (magenta lines) along Fuego and Ewan river valleys are also indicated (from Coronato *et al.*, 2008a, b). A-A' General cross section displaying the complex structure resulting from transensional faulting overprinting NE-vergent thrusts. B-B' and C-C' WNW-ESE sections shows the similar structural architecture along the northern lake margin and the submerged within the basin. Thick black line in C-C' corresponds to the longitudinal thrust projection. Profile B-B' shows the sedimentary infill covering the underlying geology.

by sub-horizontal Miocene beds of cabo Ladrillero and cabo San Pablo units (Malumián and Olivero, 2006; Ponce *et al.*, 2008; Torres-Carbonell *et al.*, 2008a). There is an evident parallelism between the general WNW-ESE orientation of LY and the strike of the local thrusts (Fig. 2). Although it cannot be fully ruled out the existence of a pre-Miocene proto-Yehuín basin, likely an intermountain depression between thrust ridges. However the configuration of the acoustic fabrics and deposit geometry does not support a syn-compressional basin formation.

5.4. Neogene transtensional regime and ice-related deposits

Information gained from seismic records indicates a transtensional regime for the basin formation, with the presence of negative flower structures, which suggests coeval strike-slip and extensional components of the deformation (Fig. 12). The activity of the interpreted transtensional fault system in LY is temporally constrained between the last pulses of compressional tectonics in the external FFTB and the time preceding the LU deposition. It is known that in Late Miocene, a transtensional regime was established along the South America-Scotia plate boundary (Eagles, 2016). The onset of major strike-slip faulting in Tierra del Fuego is considered to be not older than the Late Miocene (Torres-Carbonell *et al.*, 2014). Given that the glacial deposits of the IU fossilize the extensional structures, the transtensional activity is roughly constrained between Late Miocene and pre-Pleistocene. The Yehuín terminal moraine that currently delimits the lake to the west (Fig. 12) has been preliminarily bracketed between 25,000 and 12,100 yr B.P. (Coronato *et al.*, 2008a), which possess a time constrain for the glacial deposits within the western Yehuín basin. A minimum age for Ewan glacier lobe retreat is provided by radiocarbon dating of a peat bog within the remains of Hantuk moraine which yielded 9,300 yr B.P. (Coronato *et al.*, 2008b) indicating a probable Holocene age for glacial deposits within the Eastern sub basin. Post-glacial tectonic has been recognized for LDFS at lago Deseado area (Klepeis, 1994b; Menichetti *et al.*, 2008), which suggests a westward migration in strike-slip activity along the LDFS. Analogous age trend was also reported for the Magallanes-Fagnano Fault system (MFFS; Esteban *et al.*, 2012). NE-striking extensional faults bounding the central high and the western and

eastern lake margins (Fig. 12) may be related to reactivation of ancient transfer faults of the Jurassic extensional stage. Moreover, the overall orientation of the former Fuego and Ewan glaciers was likely controlled also by these Mesozoic structures (Fig. 13). The prominent, sharply defined shallow relief in the central part of LY forms a continuous cross-basin barrier. Substantial variations in sediment thickness occur on either side of this barrier, particularly in the intermediate unit (Fig. 8B). Such contrast may be caused either by differences in the sediment supply and/or diachronism in depocenter generation. This last possibility may be discarded given that deposits of the LU are found in both sub-basins (Fig. 8A).

The main input of sediments to the Western sub-basin during this period was due to the recessing Fuego lobe glacier, whereas for the Eastern sub-basin was the Ewan lobe glacier. One possible explanation to the differences in sedimentation rate between the two sub-basins could be ascribed to the fact that the two glaciers (Ewan and Fuego) were different in size and strength, and therefore carried out different amount of sediments. Another explanation could be that the sub-basins were deglaciated at different times, and therefore while one was free of ice and was filled up by sediments, the other one could have been under a glacier. In both cases, the position of the morphological sill helped to separate the sediment loads, causing the differences in the sedimentation rates. During the period of glacier retreat, the westernmost sub-basin was the main morphological receptacle of clastic material for the Fuego lobe. It is noteworthy that the southwards glacier route as indicated by moraine arcs displays a sharp bend from NE-SW to WNW-ESE when the recessing lobe meets the western Yehuín basin (Fig. 12). In contrast, the situation was slightly different for the Eastern sub-basin in relation to the Ewan lobe, whose recessional path met the Chepelmut basin in route to the Eastern sub-basin. It is inferred that the Chepelmut basin sequestered a significant proportion of clastic material transported by the Ewan lobe, keeping the Eastern sub basin as an underfed basin. The lack of glacial sedimentation in the central high also supports independent sedimentary histories during the glacier dominated stage. The inherited basin morphology and the differences in the behavior of glacier-lobe retreat resulted in different sedimentary architecture between both sub-basins. Western and Eastern sub basins sheared a common history only since the

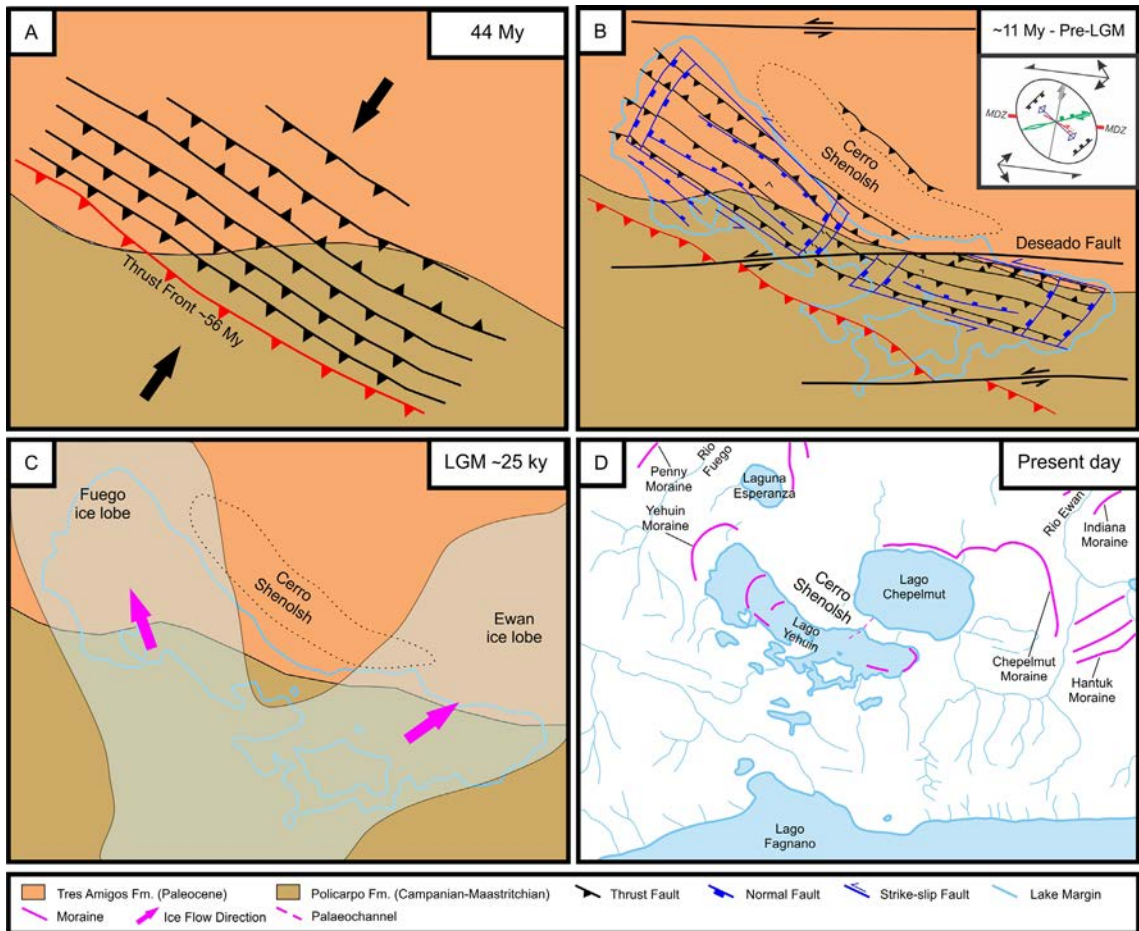


FIG. 13. Schematic reconstruction of the main evolutionary stages of the lago Yehuín basin. **A.** During Eocene times the area was set in a regional compressive scenario. The emplacement of thrust sheets began in the Ypresian and continued till the early Miocene (~56 to ~20-16 Myr); **B.** Strike-slip regime was established around 11-7 Myr. A series of normal faults were developed parallel and perpendicular with the thrust faults. The two sub-basins separated by a structural high were generated during this period. The inset shows the Riedel shear model for the Neogene deformation. MDZ: Main Deformation Zone; **C.** During the LGM (~25 kyr), the northern diffluent lobes of the Fagnano palaeoglacier, Fuego and Ewan ice lobes, flowed through the Western and Eastern sub-basins of lago Yehuín, over the deposits of the LU; **D.** The present configuration of the water bodies and the position of the recessional moraines both onland and submerged within the lacustrine basin.

lacustrine stage. In this connection, it is noteworthy that the thickest deposits of the IU are found in the westernmost sector of the Western sub-basin (Fig. 8B). The western limit of LY is currently delimited by the Yehuín terminal moraine which forms a crested topographic high of 30-70 m above lake level. The basement topography within the lake adjacent to the Yehuín moraine shows an abrupt slope in this margin (related to NE-SW extensional faults, Fig. 12) which is characterized by a relief of >120 m (Fig. 10). Therefore, the accumulated height difference >150 m

in a short distance (about 2 km) may have provided the accommodation space for the deposition of the thickest glacial sedimentary package within the LY (up to 120 m) likely in a recessional stage of the Fuego Ice lobe.

It has been long recognized that glaciers exploit previous structures as natural channels for ice flow; in particular recent studies highlighted the close relationship between the structures related to wrench kinematics in the southern Andes and fjords orientation (Glasser and Ghiglione, 2009 and references therein; Breuer *et*

al., 2013), *i.e.*, Fagnano, Beagle Channel glaciers are examples of the structural control exerted on overall glacier discharge patterns (Bujaleski, 2011; Lodolo et al., 2002, 2003). The general trend of Fuego and Ewan glaciers strongly reflects this structural control on glacial erosion; in this case the general orientation of the northern diffluent lobes of the Fagnano paleoglacier would have been governed by structures of the same strike as the Jurassic transfer faults (Fig. 12) that could have been reactivated during strike-slip tectonics. Moreover, the obstacle represented by Cerro Shenolsh and its southern prosecution, *i.e.*, the internal barrier within the LY (Fig. 12B-B', C-C'), caused the separation of the northern diffluent of Fagnano glacier in two ice lobes, Fuego and Ewan. The Yehuín sub-basins, in turn, acted as transverse depressions in the glacier route, both during advance and retreat stages forcing a sharp bend in the ice path. Therefore, the location of glacier deposits during the recessing stages, in and around LY area, were strongly controlled by both the reactivation of ancient Jurassic transfer faults as well as by localized depressions related to strike-slip faults. During this stage the lake's waters were emptied towards the Atlantic Ocean, as it is also recorded by fluvial outwash relics in the Ewan and Fuego rivers area (Coronato et al., 2005). After the glaciers retreated, the general sediment supply pattern inverted, establishing the present drainage pattern with the LY being part of the lago Fagnano watershed.

6. Conclusions

The contribution of this work is mainly focused in the analysis of newly acquired seismic data within the LY, a previously unexplored area from a geophysical point of view, located in the core of the isla Grande de Tierra del Fuego. The seismic records have been used to image the sub-bottom morphology of the basin, to derive its sedimentary architecture, and to propose an evolutionary history of the lake within the general tectonic framework of the external Magallanes fold-and-thrust belt.

The acquired data have yielded a 3-D representation of the LY basin, which is composed by two sub-basins of comparable sizes (7 km major axis, and 2-3 km minor axis) but distinct depths: the Western sub-basin reaches up to 118 m below the lake water level, whereas the Eastern sub-basin has a maximum depth of 80 m. Three seismic units are

defined within both the LY sub-basins, which reflect different sedimentation/structure relationships. Due to the lack of age information of the sedimentary infill, it is not possible to temporally correlate the interpreted sequences with the outcrop data. However, we propose here some interpretation about the evolution of the LY sedimentary fill. The poorly represented, lowermost unit (LU) is considered younger than Late Miocene in age (onset of wrenching kinematics in Tierra del Fuego), and might correspond to mass-flow deposits. The erosional activity of subsequent Pleistocene glaciations would have been responsible for the very limited deposits of the LU. The sedimentary record is dominated by the intermediate unit (IU) of glacio-lacustrine deposits (up to 120 m) with distinct thicknesses in both sub-basins, indicating separated evolutionary histories during this stage. Several moraine arcs have been interpreted, along with onland moraine ridges, allowing to reconstruct the recessional paths of Fuego and Ewan ice lobes. The entire LY basin is draped by a thin (<10 m) lacustrine unit, including the central barrier indicating the onset of a single basin since 12,000 yr B.P. Although the significant differences in basins size, the total sedimentary thickness of LY (up to 140 m) is comparable to the adjacent Lago Fagnano (up to 150 m). Their stratigraphic history is also similar in relation to glacial and lacustrine stages. There is a tight correspondence between structural lineaments and ice flow paths of Ewan and Fuego lobes. The structurally-controlled corridors of ice discharge were later reshaped by glacial activity.

Analysis and integration of geologic field data and seismic records suggest that LY is the product of a Neogene wrench kinematics overprinting pre-existing compressive structures. A left-lateral transtensional regime along WNW-ESE structures was interpreted as the responsible factor for the development of the Western and Eastern sub-basins. Internal compartment and external boundaries of LY are related to NE-SW extensional faults which reactivated old Mesozoic structures. Therefore, LY basin is interpreted as a strike slip basin developed along the major deformation zone of the Lago Desado Fault System, a main segment of the South America-Scotia plate boundary.

Acknowledgments

We acknowledge those people who contributed with field work in Tierra del Fuego: J.L. Hormaechea, G. Connon,

L. Barbero and C. Ferrer (EARG) for their support during data acquisition in the field, M. Grossi (OGS) for seismic data acquisition. Funds for this study were partly provided by the Italian Ministero degli Affari Esteri (MAE) under the project “Le variazioni climatiche del Tardo Quaternario: Uno studio sui laghi dell’Argentina meridionale”, and the MiNCyT “La Agencia” PICT 2013-2236 projects and from CONICET PIP Nro. 112201101 00618, Argentina. We are grateful for the constructive reviews made by Dr. Paterlini and Dr. Chernicoff which greatly improved the original manuscript, and the reviews made by the Editor, Dr. Vivallo.

References

- Allen, P.A.; Allen, J.R. 2005. Basin analysis: principles and applications. Blackwell Publishing: 549 p. Malden.
- Baradello, L.; Carcione, J.M. 2008. Optimal seismic-data acquisition in very shallow waters: Surveys in the Venice lagoon. *Geophysics* 73 (6): 59-63. doi: 10.1190/1.2976117.
- Breuer, S.; Kilian, R.; Schörner, D.; Weinrebe, W.; Behrmann, J.; Baeza, O. 2013. Glacial and tectonic control on fjord morphology and sediment deposition in the Magellan region (53°S), Chile. *Marine Geology* 346: 31-46.
- Bruhn, R.L. 1979. Rock structures formed during back-arc basin deformation in the Andes of Tierra del Fuego. *Geological Society of America, Bulletin* 90 (11): 998-1012.
- Bujalesky, G.G. 2011. The flood of the Beagle Valley (11,000 yr BP), Tierra del Fuego. *Anales del Instituto Patagonia* 39 (1): 5-21. doi: 10.4067/S0718-686X2011000100001.
- Bujalesky, G.G.; Heusser, C.J.; Coronato, A.M.; Roig, C.E.; Rabassa, J.O. 1997. Pleistocene glaciolacustrine sedimentation at Lago Fagnano, Andes of Tierra del Fuego, Southernmost South America. *Quaternary Science Reviews* 16 (7): 767-778.
- Caldenius, C.R.C. 1932. Las glaciaciones cuaternarias en la Patagonia y Tierra del Fuego: una investigación regional, estratigráfica y geocronológica, una comparación con la escala geocronológica sueca. *Dirección General de Minas y Geología* 95: 150 p. Buenos Aires.
- Calderón, M.; Fildani, A.; Hervé, F.; Fanning, C.M.; Weislogel, A.; Cordani, U. 2007. Late Jurassic bimodal magmatism in the northern sea-floor remnant of the Rocas Verdes basin, southern Patagonian Andes. *Journal of the Geological Society* 164 (5): 1011-1022.
- Chapron, E.; Van Rensbergen, P.; Beck, C.; De Batist, M.; Paillet, A. 1996. Lacustrine sedimentary records of brutal events in Lake Le Bourget (Northwestern Alps-Southern Jura). *Quaternaire* 7 (2-3): 155-168.
- Coronato, A.; Seppälä, M.; Rabassa, J. 2005. Last glaciation landforms in Lake Fagnano ice lobe, Tierra del Fuego, southernmost Argentina. *In International Conference on Geomorphology*, No. 6, Abstract: p. 35. Zaragoza.
- Coronato, A.; Ponce, F.; Sepälä, M.; Rabassa, J. 2008a. Englazamiento del valle del río Fuego durante el Pleistoceno tardío, Tierra del Fuego, Argentina. *In Congreso Geológico Argentino*, No. 17, Actas de resúmenes: 1194-1195. Buenos Aires.
- Coronato, A.; Ponce, F.; Rabassa, J.; Sepälä, M. 2008b. Evidencias morfológicas del englazamiento del valle del río Ewan, Tierra del Fuego, Argentina. *In Congreso Geológico Argentino*, No. 17, Actas de resúmenes: 1196-1197. Buenos Aires.
- Coronato, A.; Seppälä, M.; Ponce, J.F.; Rabassa, J. 2009. Glacial geomorphology of the Pleistocene Lake Fagnano ice lobe, Tierra del Fuego, southern South America. *Geomorphology* 112 (1-2): 67-81.
- Dalziel, I.W.D. 1982. The early (pre-Middle Jurassic) history of the Scotia arc region: a review and progress report. *Antarctic Geoscience* 13: 111-126.
- Dalziel, I.W.D. 1989. Tectonics of the Scotia Arc, Antarctica: Punta Arenas, Chile to Ushuaia, Argentina. *American Geophysical Union* 180: 206 p. doi: 10.1029/FT180.
- Dalziel, I.W.; Elliot, D.H. 1973. The Scotia Arc and Antarctic margin. *In The Ocean Basins and Margins. The South Atlantic*. Plenum Press 1: 171-245. New York.
- Dalziel, I.W.D.; Palmer, K.E. 1979. Progressive deformation and orogenic uplift at the southern extremity of the Andes. *Geological Society of America, Bulletin* 90: 259-280.
- Dalziel, I.W.D.; Brown, R.L. 1989. Tectonic denudation of the Darwin metamorphic core complex in the Andes of Tierra del Fuego, southernmost Chile: implications for Cordilleran orogenesis. *Geology* 17: 699-703.
- Dalziel, I.W.D.; de Witt, M.J.; Palmer, K.F. 1974. Fossil marginal basin in the southern Andes. *Nature* 250: 291-294.
- Diraison, M.; Cobbold, P.R.; Gapais, D.; Rossello, E.A.; Le Corre, C. 2000. Cenozoic crustal thickening, wrenching and rifting in the foothills of the southernmost Andes. *Tectonophysics* 316 (1): 91-119.
- Donda, F.; Brancolini, G.; Tosi, L.; Kovacevic, V.; Baradello, L.; Gacic, M.; Rizzetto, F. 2008. The ebb-

- tidal delta of the Venice Lagoon, Italy. *The Holocene* 18 (2): 267-278.
- Eagles, G. 2016. Tectonic reconstructions of the Southernmost Andes and the Scotia Sea during the opening of the Drake Passage. *In* *Geodynamic Evolution of the Southernmost Andes*. Springer Earth System Sciences: 75-108. doi: 10.1007/978-3-319-39727-6_4.
- Esteban, F.D.; Tassone, A.; Menichetti, M.; Rapalini, A.E.; Remesal, M.B.; Cerredo, M.E.; Lippai, H.; Vilas, J.F. 2011. Magnetic fabric and microstructures across the Andes of Tierra del Fuego, Argentina. *Andean Geology* 38 (1): 64-81. doi: 10.5027/andgeoV38n1-a05.
- Esteban, F.D.; Tassone, A.; Lodolo, E.; Menichetti, M.; 2012. The South America-Scotia plate boundary from 67°W to 56°W (Southernmost Atlantic ocean). *Rendiconti Online Società Geologica Italiana* 22: 76-79.
- Esteban, F.D.; Tassone, A.; Lodolo, E.; Menichetti, M.; Lippai, H.; Waldmann, N.; Darbo, A.; Baradello, L.; Vilas, J.F. 2014. Basement geometry and sediment thickness of Lago Fagnano (Tierra del Fuego). *Andean Geology* 41 (2): 293-313. doi: 10.5027/andgeoV41n2-a02.
- Eyles, N.; Boyce, J.I.; Halfman, J.D.; Koseoglu, B. 2000. Seismic stratigraphy of Waterton Lake, a sediment-starved glaciated basin in the Rocky Mountains of Alberta, Canada and Montana, USA. *Sedimentary Geology* 130 (3): 283-311.
- Fernández, R.; Gulick, S.; Rodrigo, C.; Domack, E.; Leventer, A. 2017. Seismic stratigraphy and glacial cycles in the inland passages of the Magallanes región of Chile, southernmost South America. *Marine Geology* 386: 19-31.
- Fuenzalida, R.H. 1972. Geological correlation between the Patagonian Andes and the Antarctic Peninsula and some tectonic implications. Master Thesis (Unpublished), Stanford University: 75 p. Stanford.
- Ghiglione, M.C.; Ramos, V.A. 2005. Progression of deformation and sedimentation in the southernmost Andes. *Tectonophysics* 405: 25-46.
- Ghiglione, M.C.; Navarrete-Rodríguez, A.T.; González-Guillot, M.; Bujalesky, G. 2013. The opening of the Magellan Strait and its geodynamic implications. *Terra Nova* 25 (1): 13-20.
- Glasser, N.; Ghiglione, M.C. 2009. Structural, tectonic and glaciological controls on the evolution of fjord landscapes. *Geomorphology* 105: 291-302.
- Hanson, R.E.; Wilson, T.J. 1991. Submarine rhyolitic volcanism in a Jurassic proto-marginal basin, southern Andes, Chile and Argentina. *In* *Andean magmatism and its tectonic setting* (Harmon, R.S.; Rapela, C.W.; editors). Geological Society of America, Special Paper 265: 13-27.
- Ingersoll, R.V.; Busby, C.J. 1995. Tectonics of sedimentary basins. *In* *Tectonics of Sedimentary Basins* (Busby, C.J.; Ingersoll, R.V.; editors), Blackwell Science: 1-52. Oxford.
- Katz, H.R. 1972. Plate tectonics-orogenic belt in the southeast Pacific. *Nature* 237: 331-332.
- Klepeis, K.A. 1994a. A relationship between uplift of the metamorphic core of the southernmost Andes and shortening in the Magallanes foreland fold and thrust belt, Tierra del Fuego. *Tectonics* 13: 882-904.
- Klepeis, K.A. 1994b. The Magallanes and Deseado fault zones: major segments of the South American-Scotia transform plate boundary in southernmost South America, Tierra del Fuego. *Journal of Geophysical Research* 99: 22001-22014.
- Klepeis, K.A.; Austin, J.A. 1997. Contrasting styles of superposed deformation in the southernmost Andes. *Tectonics* 16 (5): 755-776.
- Kraemer, P.E. 2003. Orogenic shortening and the origin of the Patagonian orocline (56°S). *Journal of South American Earth Sciences* 15: 731-748.
- Kraemer, P.E.; Introcaso, A.; Robles, A. 1996. Perfil Geológico Gravimétrico Regional a los 50° latitud Sur. Estructura Crustal y Acortamiento Andino. Cuenca Austral y Cordillera Patagónica. *In* Congreso Geológico Argentino, No. 14 y Congreso de Exploración de Hidrocarburos, No. 4, Actas 2: 423-432. Buenos Aires.
- Kranck, E.H. 1932. Geological Investigations in the Cordillera of Tierra del Fuego. *Acta Geographica* 4 (2): 1-231. Helsinki.
- Kohn, M.J.; Spear, F.S.; Harrison, T.M.; Dalziel, I.W.D. 1995. ⁴⁰Ar/³⁹Ar geochronology and P-T-t paths from the Cordillera Darwin metamorphic complex, Tierra del Fuego, Chile. *Journal of Metamorphic Geology* 13 (2): 251-270.
- Lippai, H.; Lodolo, E.; Tassone, A.; Hormaechea, J.L.; Menichetti, M.; Vilas, J.F.; TESAC Party. 2004. Morpho-structure of Lago Fagnano (Tierra del Fuego) and adjacent areas. *Bollettino di Geofisica Teorica ed Applicata* 45 (2): 142-144.
- Lodolo, E.; Menichetti, M.; Tassone, A.; Sterzai, P. 2002. Morphostructure of the central-eastern Tierra del Fuego Island from geological data and remote-sensing images. EGS Stephan Mueller, Special Publication Series 2: 1-16.
- Lodolo, E.; Menichetti, M.; Bartole, R.; Ben-Avraham, Z.; Tassone, A.; Lippai, H. 2003. Magallanes-Fagnano

- continental transform fault (Tierra del Fuego, southernmost South America). *Tectonics* 22 (6): 1076. doi: 10.1029/2003TC001500.
- Lodolo, E.; Lippai, H.; Tassone, A.; Zanolla, C.; Menichetti, M.; Hormaechea, J.L. 2007. Gravity map of the Isla Grande de Tierra del Fuego, and morphology of Lago Fagnano. *Geologica Acta* 4: 307-314.
- Lodolo, E.; Tassone, A.; Baradello, L.; Lippai, H.; Grossi, M. 2010. Morpho-Bathymetric survey of Lago Roca (Tierra del Fuego). *Bollettino di Geofisica Teorica ed Applicata* 51: 125-126.
- Lyons, R.P.; Scholz, C.; Buoniconti, M.R.; Martin, M.R. 2011. Late Quaternary stratigraphic analysis of the Lake Malawi Rift, East Africa: An integration of drill-core and seismic-reflection data. *Palaeogeography, Palaeoclimatology, Palaeoecology* 303: 20-37.
- Malumíán, N.; Olivero, E.B. 2006. El Grupo Cabo Domingo, Tierra del Fuego: bioestratigrafía, paleoambientes y acontecimientos del Eoceno-Mioceno marino. *Revista de la Asociación Geológica Argentina* 61: 139-160.
- Martinioni, D.R.; Olivero, E.B.; Medina, F.A.; Palamarczuk, S. 2013. Cretaceous stratigraphy of Sierra de Beauvoir, Fuegian Andes, Argentina. *Revista de la Asociación Geológica Argentina* 70 (1): 70-95.
- Mendoza, L.; Perdomo, R.; Hormaechea, J.L.; Del Cogliano, D.; Fritsche, M.; Richter, A.; Dietrich, R. 2011. Present-day crustal deformation along the Magallanes-Fagnano Fault System in Tierra del Fuego from repeated GPS observations. *Geophysical Journal International* 184: 1009-1022.
- Mendoza, L.; Richter, A.; Fritsche, M.; Hormaechea, J.L.; Perdomo, R.; Dietrich, R. 2015. Block modeling of crustal deformation in Tierra del Fuego from GNSS velocities. *Tectonophysics* 651-652: 58-65. doi: 10.1016/j.tecto.2015.03.013.
- Menichetti, M.; Lodolo, E.; Tassone, A.; Geletti, R. 2001. Neotectonics at the continental Transform boundary of the South America-Scotia plates: the Magallanes-Fagnano fault system. *Terra Antartica Publ "Antarctic Neotectonic" workshop*: 55 p. Siena.
- Menichetti, M.; Lodolo, E.; Tassone, A.; Hormaechea, J.L.; Lippai, H. 2007a. Geología dell'area del Lago Fagnano in Terra del Fuoco (Sud America). *Rendiconti Online Società Geologica Italiana* 4: 251-254.
- Menichetti, M.; Tassone, A.; Flores, J. 2007b. Neotectonics and seismotectonics of the Tierra del Fuego region. *In International Congress on the Geology and Geophysics of the Southern Hemisphere (Geosur), Abstracts* 127: p. 100. Punta Arenas.
- Menichetti, M.; Lodolo, E.; Tassone, A. 2008. Structural geology of the Fuegian Andes and Magallanes fold-and-thrust belt-Tierra del Fuego Island. *Geologica Acta* 6 (1): 19-42.
- Mitchum, R.M. Jr.; Vail, P.R.; Sangree, J.B. 1977. Seismic stratigraphy and global changes of sea level, part 6: seismic stratigraphic interpretation procedure. *In Seismic Stratigraphy-Applications of Hydrocarbon Exploration* (Payton, C.E.; editor). American Association of Petroleum Geologists, Memoir 26: 117-134. Tulsa.
- Nelson, E.P.; Dalziel, I.W.D.; Milnes, A.G. 1980. Structural geology of the Cordillera Darwin-collisional style orogenesis in the southernmost Chilean Andes. *Eclogae Geologicae Helveticae* 73 (3): 727-751.
- Olivero, E.B.; Martinioni, D.R. 2001. A review of the geology of the Fuegian Andes. *Journal of South American Earth Sciences* 14: 175-188.
- Olivero, E.B.; Malumíán, N. 2008. Mesozoic-Cenozoic stratigraphy of the Fuegian Andes, Argentina. *Geologica Acta* 6 (1): 5-18.
- Pinson, L.J.W.; Vardy, M.E.; Dix, J.K.; Henstock, T.J.; Bull, J.M.; Maclachlan, S.E. 2013. Deglacial history of glacial lake Windermere, UK: implications for the Central British and Irish Ice Sheet. *Journal of Quaternary Science* 28 (1): 83-94. doi: 10.1002/jqs.2595.
- Ponce, J.J.; Olivero, E.B.; Martinioni, D.R. 2008. Upper Oligocene-Miocene clinoforms of the foreland Austral Basin of Tierra del Fuego, Argentina: Stratigraphy, depositional sequences and architecture of the foredeep deposits. *Journal of South American Earth Sciences* 26 (1): 36-54.
- Pugin, A.; Pullan, S.E.; Sharpe, D.R. 1999. Seismic facies and regional architecture of the Oak Ridges Moraine area, southern Ontario. *Canadian Journal of Earth Sciences* 36: 409-432.
- Rabassa, J.; Coronato, A.; Martínez, O. 2011. Late Cenozoic glaciations in Patagonia and Tierra del Fuego: an updated review. *Biological Journal of the Linnean Society* 103 (2): 316-335.
- Schnellmann, M.; Anselmetti, F.S.; Giardini, D.; McKenzie, J.A.; Ward, S.N. 2002. Prehistoric earthquake history revealed by lacustrine slump deposits. *Geological Society of America* 30 (12): 1131-1134.
- Scholz, C.A.; Moore, T.C. Jr.; Hutchinson, D.R.; Golmshtok, A.Ja.; Klitgord, K.D.; Kuotchkin, A.G. 1998. Comparative sequence stratigraphy of low-latitude *versus* high-latitude lacustrine rift basins: seismic data examples from the East African and

- Baikal rifts. *Palaeogeography, Palaeoclimatology, Palaeoecology* 140: 401-420. doi: 10.1016/S0031-0182(98)00022-4.
- Strasser, M.; Anselmetti, F.S. 2008. Mass-movement event stratigraphy in Lake Zurich; A record of varying seismic and environmental impacts. *Beiträge zur Geologie der Schweiz, Geotechnische Serie* 95: 23-41.
- Suárez, M.; Pettigrew, T.H. 1976. An upper Mesozoic island-arc-back-arc system in the southern Andes and South Georgia. *Geological Magazine* 113 (04): 305-328.
- Suárez, M.; De la Cruz, R.; Bell, C.M. 2000. Timing and origin of deformation along the Patagonian fold and thrust belt. *Geological Magazine* 137 (4): 345-353.
- Tassone, A.; Lippai, H.; Lodolo, E.; Menichetti, M.; Comba, A.; Hormaechea, J.L.; Vilas, J.F. 2005. A geological and geophysical crustal section across the Magallanes-Fagnano fault system in Tierra del Fuego. *Journal of South American Earth Sciences* 19: 99-109.
- Tassone, A.; Santomauro, M.G.; Menichetti, M.; Cerredo, M.E.; Lodolo, E.; Remesal, M.B.; Lippai, H.; Hormaechea, J.L.; Vilas, J.F. 2011. ERT imaging of a shallow basin: Eastern Lago Fagnano, Tierra del Fuego, Argentina. *Bollettino di Geofisica Teorica ed Applicata* 52 (1): 9-21.
- Torres-Carbonell, P.J.; Dimieri, L.V. 2013. Cenozoic contractional tectonics in the Fuegian Andes, southernmost South America: a model for the transference of orogenic shortening to the foreland. *Geologica Acta* 11 (3): 359-370.
- Torres-Carbonell, P.J.; Olivero, E.B.; Dimieri, L.V. 2008a. Structure and evolution of the Fuegian Andes foreland thrust-fold belt, Tierra del Fuego, Argentina: Paleogeographic implications. *Journal of South American Earth Sciences* 25: 417-439.
- Torres-Carbonell, P.J.; Olivero, E.B.; Dimieri, L.V. 2008b. Control en la magnitud de desplazamiento de rumbo del Sistema Transformante Fagnano, Tierra del Fuego, Argentina. *Revista Geológica de Chile* 35 (1): 63-77. doi: 10.4067/S0716-02082008000100003.
- Torres-Carbonell, P.J.; Dimieri, L.V.; Olivero, E.B. 2011. Progressive deformation of a Coulomb thrust wedge: the eastern Fuegian Andes thrust-fold belt. *In Kinematic evolution and structural styles of fold-and-thrust belts* (Poblet, J.; Lisle, R.; editors). Geological Society, Special Publications 349: 123-147. London.
- Torres-Carbonell, P.J.; Dimieri, L.V.; Martinioni, D.R. 2013. Early foreland deformation of the Fuegian Andes (Argentina): constraints from the strain analysis of Upper Cretaceous-Danian sedimentary rocks. *Journal of Structural Geology* 48: 14-32.
- Torres-Carbonell, P.J.; Dimieri, L.V.; Olivero, E.B.; Bohoyo, F.; Galindo-Zaldívar, J. 2014. Structure and tectonic evolution of the Fuegian Andes (southernmost South America) in the framework of the Scotia Arc development. *Global and Planetary Change* 123 (B): 174-188.
- Waldmann, N.; Aríztegui, D.; Anselmetti, F.S.; Austin, J.A.Jr.; Dunbar, R.B.; Moy, C.M.; Recasens, C. 2008. Seismic stratigraphy of Lago Fagnano sediments (Tierra del Fuego, Argentina)-a potential archive of Paleoclimatic change and tectonic activity since the Late Glacial. *Geologica Acta* 6: 101-110.
- Waldmann, N.; Aríztegui, D.; Anselmetti, F.S.; Austin, J.A.Jr.; Dunbar, R.B.; Moy, C.M.; Recasens, C. 2009. Holocene climatic fluctuations and positioning of the Southern Hemisphere westerlies in Tierra del Fuego (54°S), Patagonia. *Journal Quaternary Sciences* 25 (7): 1063-1073.
- Waldmann, N.; Aríztegui, D.; Anselmetti, F.S.; Coronato, A.; Austin, J.A.Jr. 2010a. Geophysical evidence of multiple glacier advances in Lago Fagnano (54°S), southernmost Patagonia. *Quaternary Science Review* 29: 1188-1200.
- Waldmann, N.; Anselmetti, F.S.; Aríztegui, D.; Austin, J.A.Jr.; Pirouz, M.; Moy, C.M.; Dunbar, R. 2010b. Holocene mass-wasting events in Lago Fagnano, Tierra del Fuego (54°S): implications for paleoseismicity of the Magallanes-Fagnano transform fault. *Basin Research* 23 (2): 171-190.
- Waldmann, N.; Anselmetti, F.S.; Aríztegui, D.; Austin, J.A.Jr.; Pirouz, M.; Moy, C.M.; Dunbar, R. 2011. Holocene mass-wasting events in Lago Fagnano, Tierra del Fuego (54°S): implications for paleoseismicity of the Magallanes-Fagnano transform fault. *Basin Research* 23: 171-190.
- Wessel, P.; Smith, W.H.F. 1991. Free software helps map and display data. *EOS Transactions American Geophysical Union* 72 (41): 441-446.
- Wilson, T.J. 1991. Transition from back-arc to foreland basin development in the southernmost Andes: Stratigraphic record from the Ultima Esperanza District, Chile. *Geological Society of America, Bulletin* 103 (1): 98-111.
- Winslow, M.A. 1982. The structural evolution of the Magallanes Basin and neotectonics in the southernmost Andes. *In Antarctic Geoscience*. Madison (Craddock, C.; editor). University of Wisconsin Press: 143-154.
- Zanolla, C.; Lodolo, E.; Lippai, H.; Tassone, A.; Menichetti, M.; Baradello, L.; Grossi, M.; Hormaechea, J.L. 2011. Bathimetric map of Lago Fagnano (Tierra del Fuego Island). *Bollettino di Geofisica Teorica ed Applicata* 52: 1-8.